RESULTS

Effect of roxithromycin on T cell proliferation through different costimulatory pathways. As shown in Figure 1, CD3 stimulation alone resulted in the induction of low levels of T cell proliferation. Marked T cell proliferation was observed with CD3 stimulation in combination with an additional second signal, such as anti-CD26 Mab, anti-CD28 Mab, or PMA. Under these conditions, RXM did not inhibit T cell proliferation from different donors at virtually any concentration tested (1.4 to 28 μM). It should be noted that at higher concentration (28 μM), only slight inhibition of T cell proliferation was observed in certain donors.

Effect of roxithromycin on Th1-type and Th2-type cytokine production through different costimulatory pathways. As shown in Figure 2A, RXM, even at 28 μM, did not inhibit IL-2 production under all costimulatory conditions. In addition to IL-2, RXM did not show any apparent effect on the production of IFN-γ at any concentrations tested (1.4 to 28 μM; Figure 2A).

Since Th2-type CD4+ T cells may play a role in allergic disorders such as asthma[25,26], we next examined the effect of RXM on Th2-type cytokine production. As shown in Figure 2A, RXM did not inhibit IL-4 and IL-5 production under each costimulatory condition at any tested doses (1.4 to 28 μM). Our results therefore indicated that RXM did not inhibit Th1-type and Th2-type cytokine production in our experimental systems.

Effect of roxithromycin on proinflammatory cytokine production through different costimulatory pathways. We next examined the effect of RXM on the production of proinflammatory cytokines. As shown in Figure 2B, production of the proinflammatory cytokines IL-6 and TNF-α was significantly inhibited by RXM in a dose-dependent manner under each costimulatory condition. Therefore RXM inhibited proinflammatory cytokine productions by T cells stimulated by our costimulatory conditions.

Effect of RXM on proinflammatory cytokine production by macrophages. Since macrophages play a role in host defense against infection and in the local modulation of immune and inflammatory responses[27], we also examined the effect of RXM on the production of proinflammatory cytokines by macrophages. The preliminary time-course

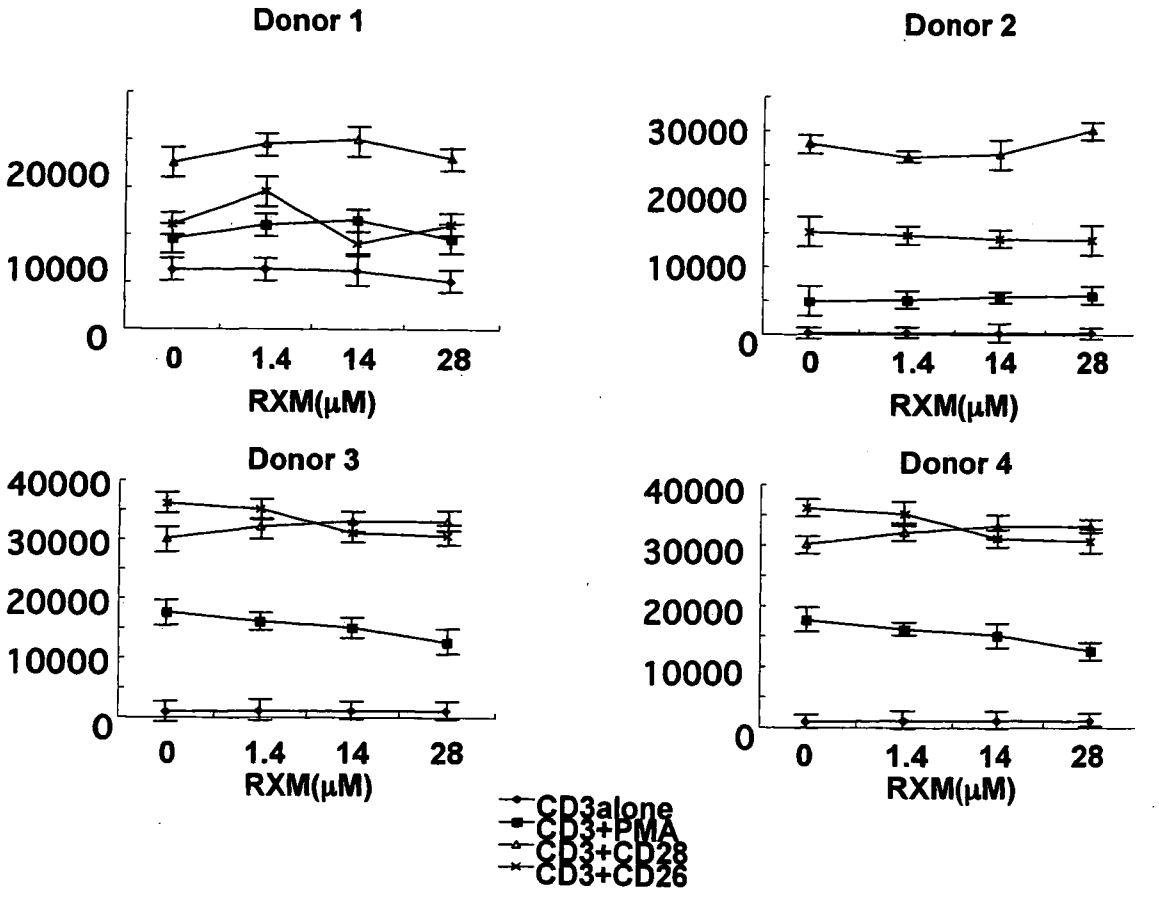

Figure 1. Effect of RXM on the proliferative response of peripheral T cells stimulated with anti-CD3 Mab alone, anti-CD3 Mab plus PMA, anti-CD3 plus anti-CD28 (4B10) Mab, and anti-CD3 plus anti-CD26 (1F7) Mab. Counts per minute (cpm) value in the case of nonstimulated T cells was near background level (data not shown). Mean cpm values ± SD from triplicate samples from 4 different donors are shown. RXM did not significantly inhibit proliferative response of T cells induced by the stimuli described above.

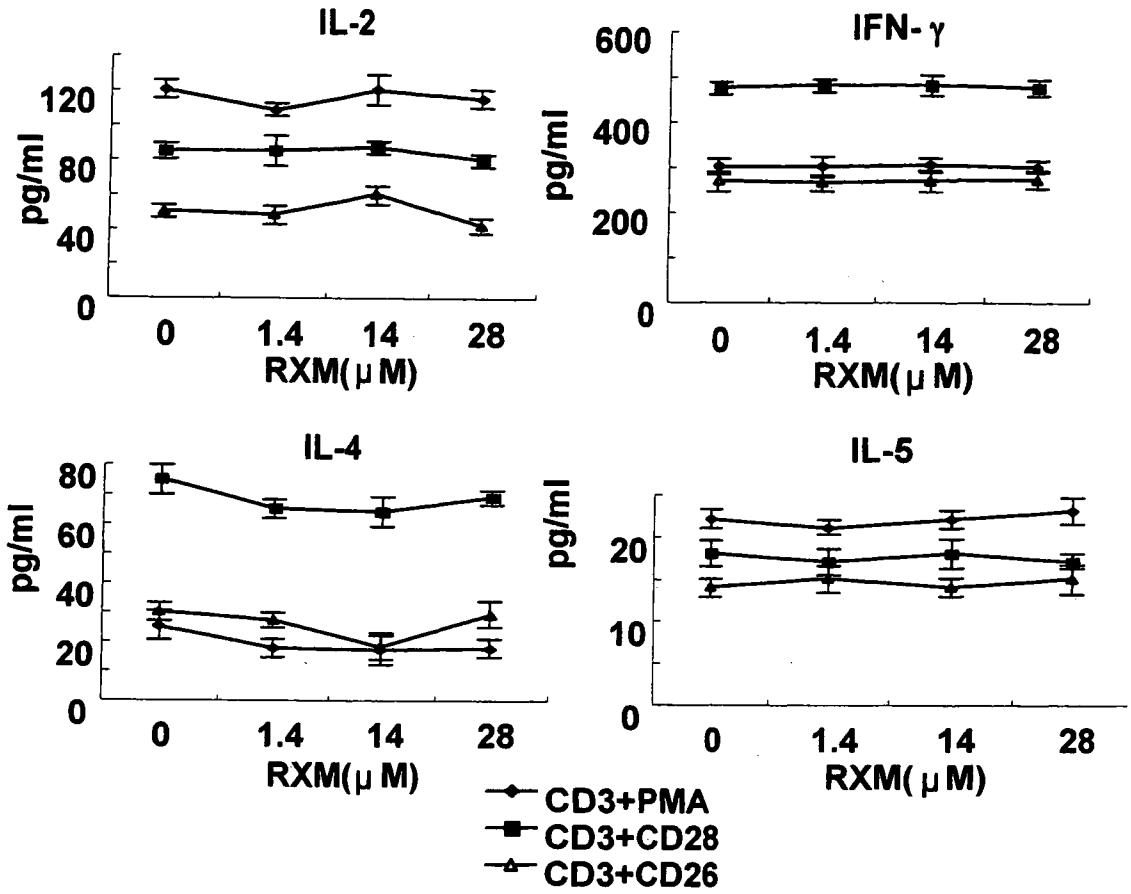

Figure 2A. Effect of RXM on peripheral T cell production of IL-2, IFN-γ, IL-4, and IL-5. T cells were stimulated with anti-CD3 plus PMA, CD3 plus CD28, and anti-CD3 plus anti-CD26 for 24 h, and culture supernatants were assayed by ELISA for cytokine levels shown here. Cytokine levels of T cells stimulated with anti-CD3 alone were always the background level (data not shown). Mean values ± SD from triplicate samples are shown; data are representative of 3 independent experiments.

experiment showed that 8 hours after stimulation was optimal for LPS-stimulated proinflammatory cytokine production by macrophages. As shown in Figure 2C, RXM inhibited both IL-6 and TNF-α production by macrophages in a dose-dependent manner.

Effect of RXM on transendothelial migration of activated T cells. We next examined its effect on transendothelial migration of PHA-stimulated T cells. These preactivated T cells spontaneously migrate from the upper chamber to the lower chamber through the endothelial monolayer, which is therefore regarded as chemokinesis. As shown in Figure 3, T cell migration was significantly inhibited in a range from 14 to 28 μM in a dose-dependent manner when RXM was present during the endothelial migration assay ($p < 0.05$). Compared to proinflammatory cytokine production by T cells and macrophages, RXM at dose of 1.4 μM did not inhibit migration of T cells from 5 different donors; but from 14 to 28 μM RXM, T cell migration was always inhibited. In contrast, when we pretreated HUVEC with various concentrations of RXM for 48 hours, and then HUVEC were washed and exposed to PHA-stimulated T cells, RXM did not affect the migration of T cells through HUVEC even at the highest concentration tested (28 μM; data not shown).

Effect of RXM therapy on the development of CIA. Finally, we investigated whether RXM affects the pathophysiology of CIA. Oral treatment of RXM was started after the second immunization of type II collagen, and daily treatment of RXM was continued up to Day 14. As shown in Figure 4, disease scores were suppressed in a dose-dependent manner after 7 days of treatment. In mice treated with RXM at a dose of 100, 200, 400, and 800 μg and control mice, statistically significant differences in disease score suppression were observed ($p < 0.05$ and $p < 0.01$). It should be noted that in the groups of mice treated with RXM 400 μg/day and 800 μg/day, disease scores were markedly inhibited, but the differences in the disease scores between the 2 groups did not reach statistical significance differences after 14 days of treatment. These results therefore indicate that RXM treatment inhibited the development of CIA.

Effect of RXM treatment on serum levels of IL-6, TNF-α, IL-4, and IFN-γ and type II collagen antibody levels. Since IL-6 and TNF-α appear to be involved in the development of

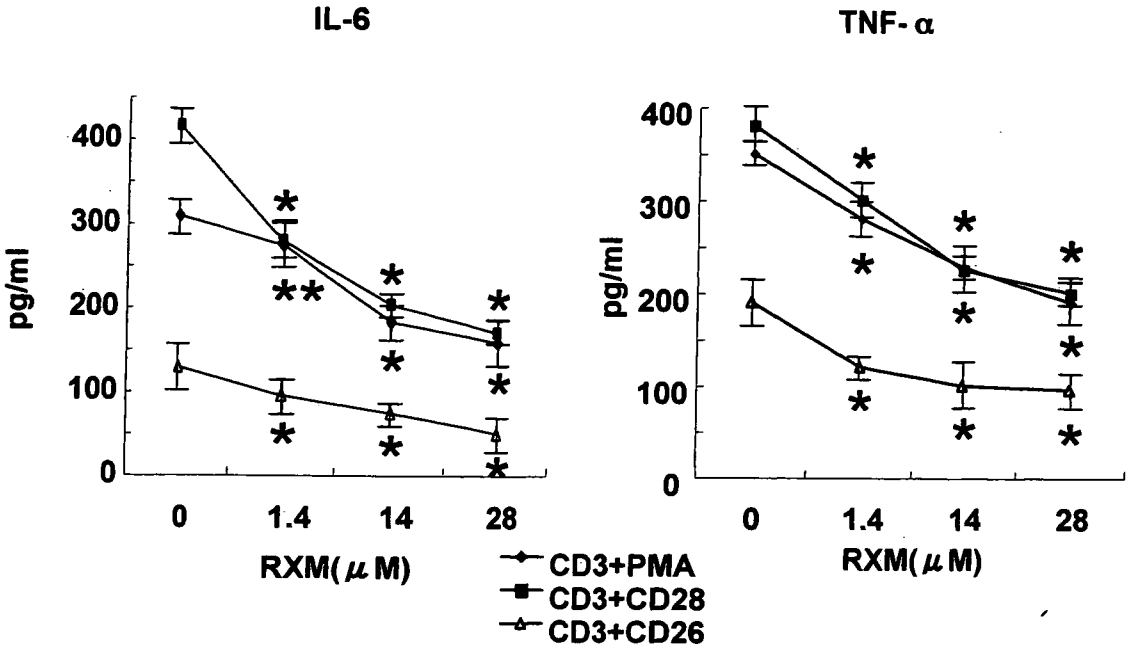

Figure 2B. Effect of RXM on peripheral T cell production of IL-6 and TNF-α. T cells were stimulated by the same conditions as in (A), and culture supernatants were assayed by ELISA for IL-6 and TNF-α. Cytokine levels of T cells stimulated with anti-CD3 alone were always the background level (data not shown). Mean values ± SD from triplicate samples are shown; data are representative of 3 independent experiments. *p <0.01, **p < 0.05 between 0 and 1.4 μM, 0 and 14 μM, 0 and 28 μM RXM; 2-tailed Student t test.

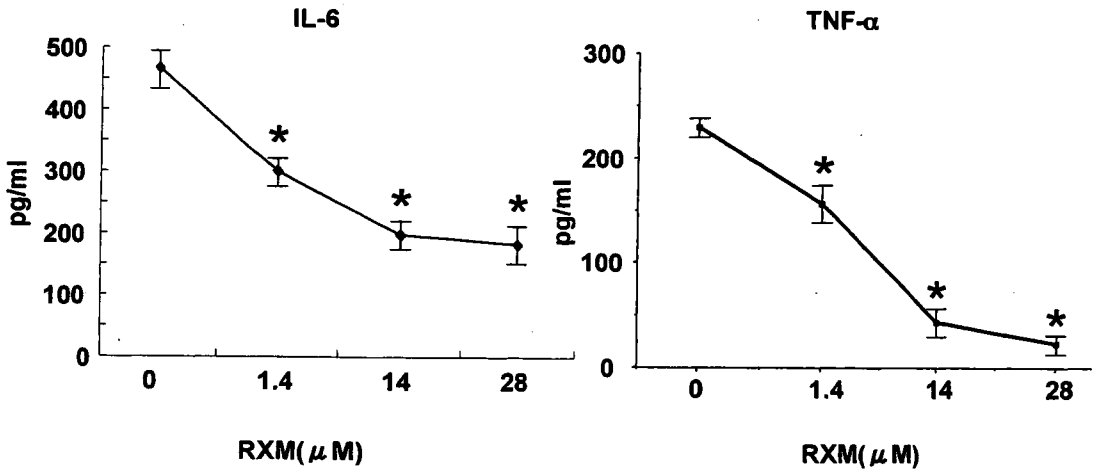

Figure 2C. Effect of RXM on production of IL-6 and TNF-α by macrophages stimulated with LPS (1 μg/ml) for 8 h; culture supernatants were assayed by ELISA for IL-6 and TNF-α. Mean values ± SD from triplicate samples are shown; data are representative of 3 independent experiments. *p <0.01 between 0 and 1.4 μM, 0 and 14 μM, 0 and 28 μM RXM; 2-tailed Student t test.

CIA[28], we examined the serum levels of those proinflammatory cytokines as well as IFN-γ and IL-4 in CIA mice on Days 0, 7, 14, and 21 after RXM treatment. While treatment of RXM did not affect the serum level of IFN-γ (Figure 5A), serum IL-6 levels increased in control CIA mice on Day 7, and then decreased to an undetectable level by Day 14. In contrast, in RXM-treated CIA mice, serum IL-6 levels were reduced on Day 7 in a dose-dependent manner. Particularly in CIA mice treated with 400 μg and 800 μg RXM, serum IL-6 levels were significantly reduced on Day 7 ($p < 0.05$; Figure 5B).

Serum IL-4 and TNF-α levels could not be detected in these groups of CIA mice due to the low degree of sensitivity of the available detection kits. Regarding type II collagen antibody levels (Figure 5C), a type II collagen antibody was detected after Day 7 of the second immunization of collagen, but RXM treatment did not affect the serum titer of this antibody. Thus we concluded that RXM treatment, particu-

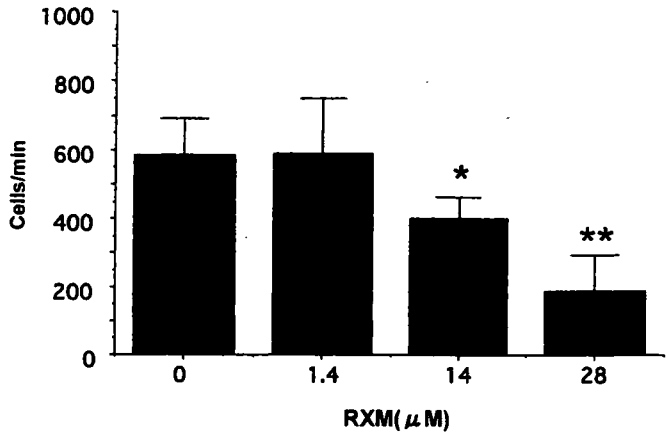

Figure 3. Inhibitory effect of RXM on transendothelial migration (chemokinesis) of PHA-activated T cells, as described in Materials and Methods. Bars show mean values ± SD of triplicate cultures. *p < 0.05 between 0 and 14 μM RXM, **p < 0.01 between 0 and 28 μM RXM; 2-tailed Student t test. Data are representative of samples from 5 different donors.

larly at the higher dose levels 400 μg and 800 μg, significantly inhibited the production of IL-6 in the serum of CIA mice.

RXM inhibition of leukocyte migration and bone destruction in affected joints of CIA mice. Histological analysis of inflamed joints and synovial tissue from those mice revealed large numbers of cells of leukocyte origin, synovial membrane proliferation, and pannus formation as well as destruction of bone and cartilage in control CIA mice not treated with RXM (Figure 6). On the other hand, in CIA mice treated with 200 and 800 μg RXM per day, the infiltration of leukocytes, cartilage and bone destruction, and pannus formation were strongly suppressed in a dose-dependent manner (Figure 6). Especially in 800 μg RXM-treated CIA mice, no cartilage and bone destruction, pannus formation, and synovial membrane proliferation was observed. These results indicated that RXM inhibited leukocyte migration as well as cartilage and bone destruction.

DISCUSSION

We demonstrated that RXM clearly inhibited the production of the proinflammatory cytokines TNF-α and IL-6 by activated T cells and macrophages. In addition, RXM inhibited T cell migration. Most importantly, RXM treatment of CIA mice inhibited the development of CIA, serum IL-6 levels, the migration of leukocytes into affected joints, and the destruction of bone and cartilage.

Previous studies showed that RXM could not inhibit concanavalin A (ConA)-induced T cell proliferation, but could inhibit ConA-induced IL-2 and IL-4 production by T cells[15]. Moreover, the same investigators reported that RXM inhibited production of Th2-type cytokine IL-4 and IL-5 but not Th1-type cytokine IL-2 and IFN-γ by T cells stimulated with the same costimulatory stimuli used in our study[29]. Although the precise reasons for the discrepancy between our findings and their data are unclear, it may be due to differences in the methods used for stimulation. Moreover, other researchers reported that other macrolides such as midecamycin, clarithromycin, and josamycin inhibited production of both Th1-type and Th2-type cytokines, such as IL-2, IL-4, and IL-5, by ConA-stimulated T cells[30]. Meanwhile, erythromycin and RXM inhibited TNF-α pro-

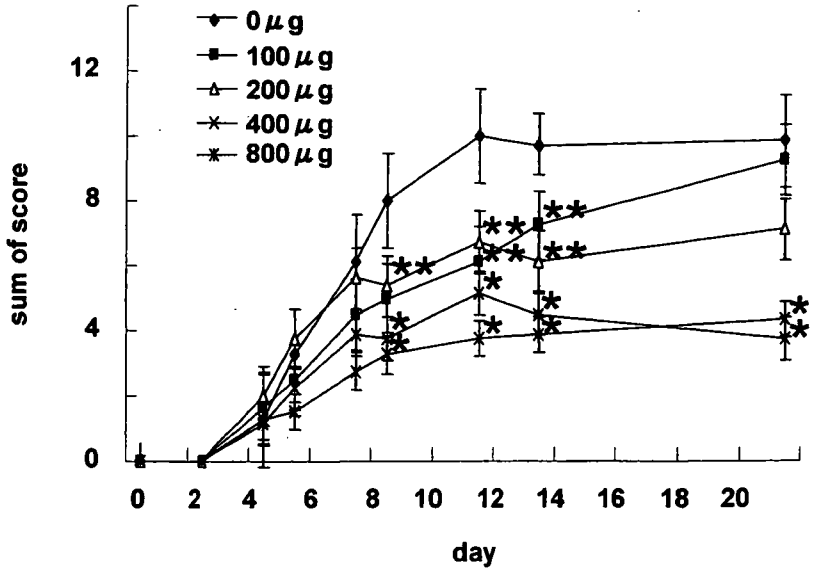

Figure 4. Effect of RXM therapy on development of CIA. Disease scores of CIA mice measured from Day 0 to Day 21 after the second immunization. Sums of scores are shown for 4 different doses of RXM (100, 200, 400, 800 μg; n = 8 for each group) and control group (n = 8). Mean values ± SD from 8 mice are plotted. *p < 0.01, **p < 0.05 between 0 and 100, 200, 400, 800 μg/day; 2-tailed Student t test.

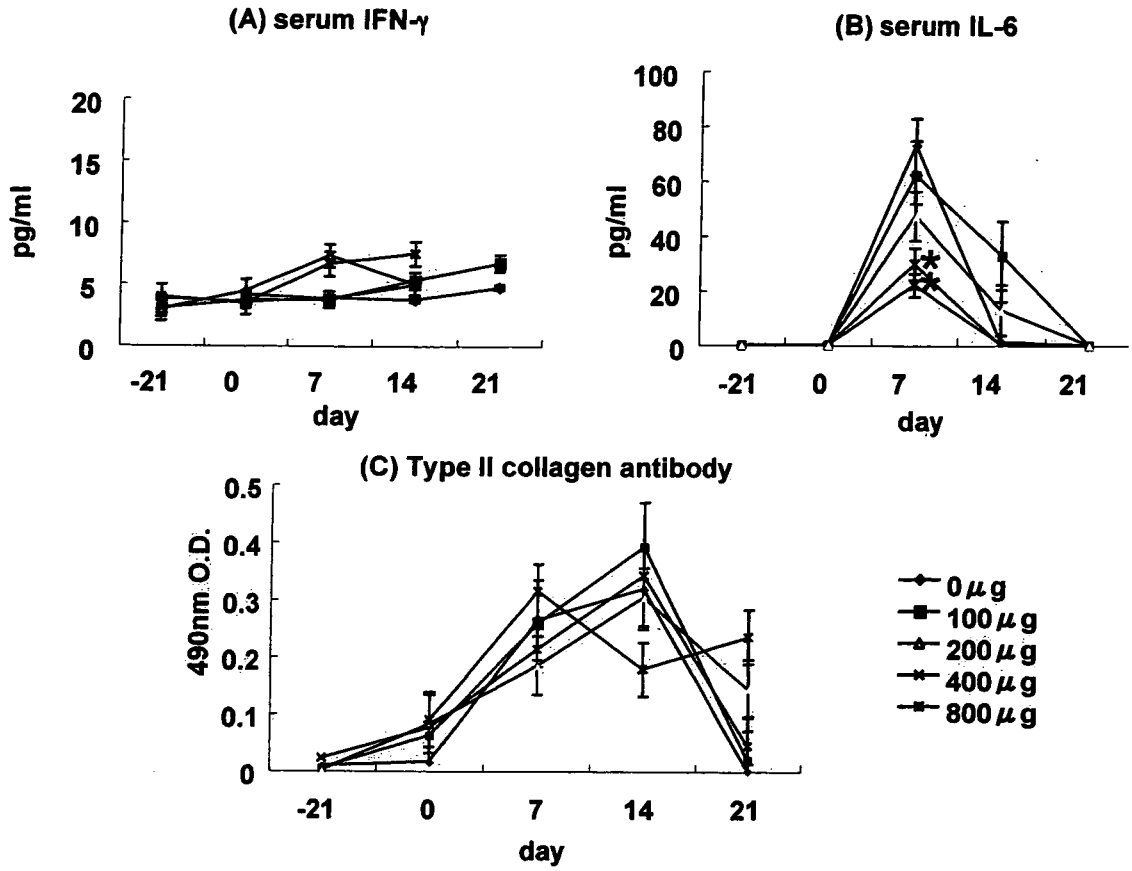

Figure 5. Effect of RXM treatment on serum levels of IFN-γ, IL-6, and type II collagen antibody in CIA mice, as described in Materials and Methods. Serum levels were plotted from 4 different doses of RXM (100, 200, 400, 800 μg; n = 8 for each group) and controls (n = 8). Mean values ± SD from 8 mice were plotted. IL-4 and TNF-α levels were always below background levels (data not shown). *$p < 0.05$, 0 versus 400 and 800 μg/day; 2-tailed Student t test.

duction by macrophages stimulated with LPS[31,32]. Recently, Guchelaar, *et al* reported that erythromycin inhibited TNF-α and IL-6 production induced by heat-killed *Streptococcus pneumoniae* in human whole blood *ex vivo*[33].

Systemic administration of macrolide antibiotics (erythromycin and RXM) has been shown to be effective in the treatment of lower and upper airway inflammatory diseases such as bronchial asthma and diffuse panbronchiolitis[2,32-34]. Although these inflammatory diseases have been reported to be successfully treated with low dose administration of macrolide antibiotics, which cannot be expected to act as antibacterial agents, the precise mechanisms of action to explain the clinical effectiveness of this therapy are not well understood. It was recently reported that bronchial asthma is a T cell-mediated inflammatory disorder, and selective recruitment of CD4+ T cells into sites of inflammation may contribute to the development of different pathological conditions[35,36]. Current studies suggest that TNF-α may potentially be involved in the development of bronchial hyperresponsiveness by directly altering the contractile properties of the airway smooth muscle[37,38]. As a regulator of IgE synthesis, increased levels of IL-6 have been detected in blood and bronchoalveolar lavage after bronchial challenge of patients with asthma, while bronchial biopsies of these patients reveal increased expression of IL-6[39]. Thus, inhibition of TNF-α and IL-6 production by T cells and macrophages as well as inhibition of T cell migration by RXM may also have important therapeutic implications for bronchial asthma.

In both CIA and RA, joint inflammation and cartilage and bone destruction depend on the concentrations of TNF-α and IL-6 in affected joints[28,40]. At the site of inflammation in the affected RA synovium, infiltration of leukocytes, especially T cells from blood vessels, is the initial step necessary for the development of the RA lesion. The *in vivo* effectiveness of RXM in preventing CIA development is likely linked to the ability of RXM to inhibit T cell migration and proinflammatory cytokine production by T cells and macrophages *in vitro*.

Based on the pharmacokinetics data in rats, oral administration of RXM at 5 mg/kg, which corresponds to 100 μg/mouse, resulted in the maximum plasma concentration around 1.9 μg/ml (2.3 μM). The usual dose in humans, 300 mg/adult, resulted in the maximum plasma concentration

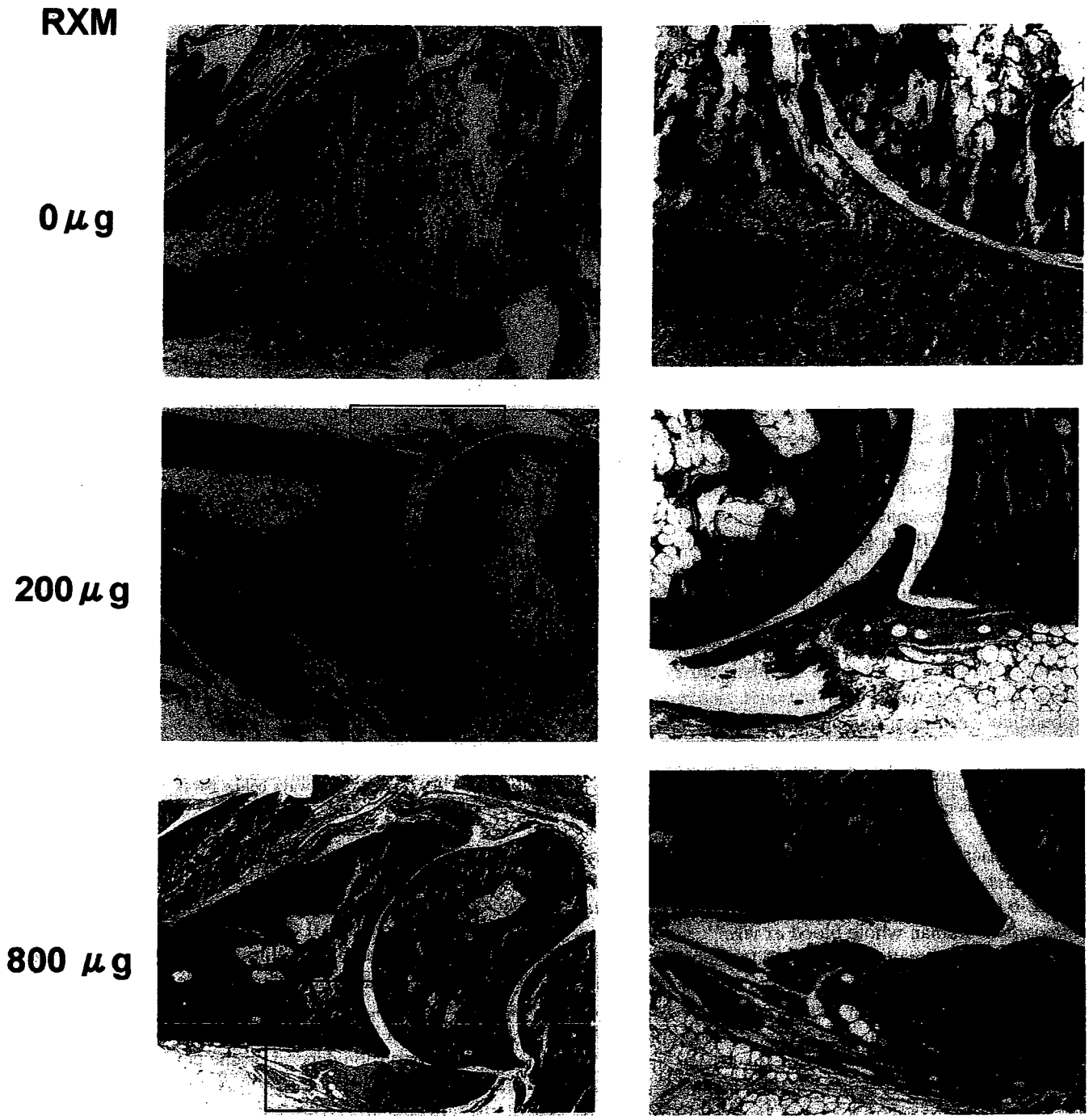

Figure 6. Ankle joints of CIA mice were collected on Day 21 after the second immunization of collagen. Mice had been treated with 0, 200, and 800 μg RXM. H&E stain; original magnification ×40 (left panels) and ×100 (right panels).

around 8.1 μg/ml (9.6 μM). Therefore, the *in vivo* concentration of RXM may correspond to the concentration that inhibits immune/inflammatory phenomena *in vitro*. Further, the doses employed in our *in vitro* and *in vivo* experiments correspond to the human daily dose.

Advances in understanding the pathogenesis of RA based on studies of human tissues and animal models of disease have led to identification of molecular targets for immunotherapeutic intervention. Of these, TNF-α has been validated as an appropriate target for treatment, and to date 2 biological agents that target TNF-α have been licensed for clinical use[40]. These are infliximab, an anti-TNF-α Mab[41], and etanercept, an engineered p75 TNF receptor dimer linked to the Fc portion of human IgG1[42]. Therapies inhibiting TNF-α in patients with active RA result in rapid and sustained improvement in symptoms and signs of disease, improve-

ment in the quality of life, and protection of joints from structural damage[40,43]. Moreover, anti-TNF-α treatment has been reported to be effective in Crohn's disease[44]. IL-6 regulates the production of acute-phase proteins by hepatocytes and activates osteoclasts to absorb bone[45,46]. In a preclinical study, a humanized anti-IL-6R Mab has been used to treat patients with severe RA, and clinical improvements have been reported[47].

Besides bronchial asthma, RA, and Crohn's disease, RXM may also be useful for the treatment of disorders in which TNF-α and IL-6 may play a role in pathophysiology, such as graft versus host disease (GVHD) following allogeneic bone marrow transplant[48], heart failure[49], and Castleman's disease[50].

ACKNOWLEDGMENT

The authors thank Fumiki Nojima for excellent secretarial assistance.

REFERENCES

1. Nelson S, Summer WR, Terry PB, Warr GA, Jakab GJ. Erythromycin-induced suppression of pulmonary antibacterial defenses. A potential mechanism of superinfection. Am Rev Respir Dis 1987;136:1207-12.
2. Kadota J, Sakito O, Kohno S, et al. A mechanism of erythromycin treatment on patients with diffuse panbronchiolitis. Am Rev Respir Dis 1993;147:153-9.
3. Miyatake H, Suzuki K, Taki F, Takagi K, Satake T. Effect of erythromycin on bronchial hyperresponsiveness in patients with bronchial asthma. Arzneimittelforschung 1991;41:552-6.
4. Yokota T, Suzuki E, Arai K. Cefpodoxime proxetil, its in vitro antibacterial activity, affinity to bacterial penicillin-binding proteins, and synergy of bactericidal activity with serum complement and mouse-cultured macrophages. Drugs Exp Clin Res 1988;14:495-500.
5. Fraschini F, Scaglione F, Ferrara F, Marelli O, Braga PC, Teodori F. Evaluation of the immunostimulating activity of erythromycin in man. Chemotherapy 1986;32:286-90.
6. Mikasa K, Sawaki M, Konishi M, et al. The effect of erythromycin treatment on natural killer cell activity in patients with chronic lower respiratory tract infections. Kansenshogaku Zasshi 1989;63:811-5.
7. Ras GJ, Anderson R, Eftychis HA, et al. Chemoprophylaxis with erythromycin stearate or amoxycillin in patients with chronic bronchitis — effects on cellular and humoral immune functions. S Afr Med J 1984;66:955-8.
8. Aho P, Mannisto PT. Effects of two erythromycins, doxycycline and phenoxymethylpenicillin, on human leucocyte chemotaxis in vitro. J Antimicrob Chemother 1988;21:29-32.
9. Anderson R. Erythromycin and roxithromycin potentiate human neutrophil locomotion in vitro by inhibition of leukoattractant-activated superoxide generation and autooxidation. J Infect Dis 1989;159:966-73.
10. Yoshimura T, Kurita C, Yamazaki F, et al. Effect of roxithromycin on proliferation of peripheral blood mononuclear cells and production of lipopolysaccharide-induced cytokines. Biol Pharm Bull 1995;18:876-81.
11. Young RA, Gonzalez JP, Sorkin EM. Roxithromycin. A review of its antibacterial activity, pharmacokinetic properties and clinical efficacy. Drugs 1989;37:8-41.
12. Noma T, Hayashi M, Yoshizawa I, Aoki K, Shikishima Y, Kawano Y. A comparative investigation of the restorative effects of roxithromycin on neutrophil activities. Int J Immunopharmacol 1998;20:615-24.
13. Wakita H, Tokura Y, Furukawa F, Takigawa M. The macrolide antibiotic roxithromycin suppresses IFN-gamma-mediated immunological functions of cultured normal human keratinocytes. Biol Pharm Bull 1996;19:224-7.
14. Konno S, Adachi M, Asano K, Okamoto K, Takahashi T. Inhibition of human T-lymphocyte activation by macrolide antibiotic roxithromycin. Life Sci 1992;51:L231-6.
15. Konno S, Asano K, Kurokawa M, Ikeda K, Okamoto K, Adachi M. Antiasthmatic activity of a macrolide antibiotic, roxithromycin: analysis of possible mechanisms in vitro and in vivo. Int Arch Allergy Immunol 1994;105:308-16.
16. Robey E, Allison JP. T-cell activation: integration of signals from the antigen receptor and costimulatory molecules. Immunol Today 1995;16:306-10.
17. Green JM, Noel PJ, Sperling AI, et al. Absence of B-7 dependent responses in CD28-deficient mice. Immunity 1994;1:501-8.
18. Gimmi CD, Freeman GJ, Gribben JG, et al. B-cell surface antigen B7 provides a costimulatory signal that induces T cells to proliferate and secrete interleukin 2. Proc Natl Acad Sci USA 1991;88:6575-9.
19. Morimoto C, Torimoto Y, Levinson G, et al. 1F7, a novel cell surface molecule, involved in helper function of CD4 cells. J Immunol 1989;143:3430-9.
20. Dang NH, Torimoto Y, Deusch K, Schlossman SF, Morimoto C. Comitogenic effect of solid-phase immobilized anti-1F7 on human CD4 T cell activation via CD3 and CD2 pathways. J Immunol 1990;144:4092-100.
21. Tanaka T, Kameoka J, Yaron A, Schlossman SF, Morimoto C. The costimulatory activity of the CD26 antigen requires dipeptidyl peptidase IV enzymatic activity. Proc Natl Acad Sci USA 1993;90:4586-90.
22. Hafler DA, Fox DA, Manning ME, Schlossman SF, Reinherz EL, Weiner HL. In vivo activated T lymphocytes in the peripheral blood and cerebrospinal fluid of patients with multiple sclerosis. N Engl J Med 1985;312:1405-11.
23. Iwata S, Yamaguchi N, Munakata Y, et al. CD26/dipeptidyl peptidase IV differentially regulates the chemotaxis of T cells and monocytes toward RANTES: possible mechanism for the switch from innate to acquired immune response. Int Immunol 1999;11:417-26.
24. Rosloniec EF, Cremer M, Kang A, Myers LK. Collagen-induced arthritis. In: Coligan JE, Kruisbeek AM, Margulies DH, Shevach EM, Strober W, editors. Current protocols in immunology. New York: Wiley; 1996:15.5.1-24.
25. Kapsenberg ML, Wierenga EA, Bos JD, Jansen HM. Functional subsets of allergen-reactive human CD4+ T cells. Immunol Today 1991;12:392-5.
26. Romagnani S. Lymphokine production by human T cells in disease states. Annu Rev Immunol 1994;12:227-57.
27. Johnston RB Jr. Current concepts: immunology. Monocytes and macrophages. N Engl J Med 1988;318:747-52.
28. Marinova-Mutafchieva L, Williams RO, Mason LJ, Mauri C, Feldmann M, Maini RN. Dynamics of proinflammatory cytokine expression in the joints of mice with collagen-induced arthritis. Clin Exp Immunol 1997;107:507-12.
29. Asano K, Kamakazu K, Hisamitsu T, Suzaki H. Modulation of Th2 type cytokine production from human peripheral blood leukocytes by a macrolide antibiotic, roxithromycin, in vitro. Int Immunopharmacol 2001;11:1913-21.
30. Morikawa K, Zhang J, Nonaka M, Morikawa S. Modulatory effect of macrolide antibiotics on the Th1- and Th2-type cytokine production. Int J Antimicrob Agents 2002;19:53-9.
31. Suzaki H, Asano K, Ohki S, Kanai K, Mizutani T, Hisamitsu T.

Suppressive activity of a macrolide antibiotic, roxithromycin, on pro-inflammatory cytokine production in vitro and in vivo. Mediators Inflamm 1999;8:199-204.
32. Iino Y, Toriyama M, Kudo K, Natori Y, Yuo A. Erythromycin inhibition of lipopolysaccharide-stimulated tumor necrosis factor alpha production by human monocytes in vitro. Ann Otol Rhinol Laryngol Suppl 1992;157:16-20.
33. Guchelaar HJ, Schultz MJ, van der Poll T, Koopmans RP. Pharmacokinetic-pharmacodynamic modeling of the inhibitory effect of erythromycin on tumour necrosis factor-alpha and interleukin-6 production. Fundam Clin Pharmacol 2002;15:419-24.
34. Itkin IH, Menzel ML. Pharmacokinetic-pharmacodynamic modeling of the inhibitory effect of erythromycin on tumour necrosis factor-alpha and interleukin-6 production. J Allergy 1970;45:146-62.
35. Robinson DS, Hamid Q, Ying S, et al. Predominant TH2-like bronchoalveolar T-lymphocyte population in atopic asthma. N Engl J Med 1992;326:298-304.
36. Ying S, Humbert M, Barkans J, et al. Expression of IL-4 and IL-5 mRNA and protein product by CD4+ and CD8+ T cells, eosinophils, and mast cells in bronchial biopsies obtained from atopic and nonatopic (intrinsic) asthmatics. J Immunol 1997;158:3539-44.
37. Baeuerle PA, Henkel T. Function and activation of NF-kappa B in the immune system. Annu Rev Immunol 1994;12:141-79.
38. Amrani Y, Chen H, Panettieri RA Jr. Activation of tumor necrosis factor receptor 1 in airway smooth muscle: a potential pathway that modulates bronchial hyper-responsiveness in asthma? Respir Res 2000;1:49-53.
39. Hirano T. Interleukin 6 and its receptor: ten years later. Int Rev Immunol 1998;16:249-84.
40. Harris ED Jr. Rheumatoid arthritis. Pathophysiology and implications for therapy. N Engl J Med 1990;322:1277-89.
41. Knight DM, Trinh H, Le J, et al. Construction and initial characterization of a mouse-human chimeric anti-TNF antibody. Mol Immunol 1993;30:1443-53.
42. Weinblatt ME, Kremer JM, Bankhurst AD, et al. A trial of etanercept, a recombinant tumor necrosis factor receptor:Fc fusion protein, in patients with rheumatoid arthritis receiving methotrexate. N Engl J Med 1999;340:253-9.
43. Lipsky PE, van der Heijde DM, St. Clair EW, et al. Infliximab and methotrexate in the treatment of rheumatoid arthritis. Anti-Tumor Necrosis Factor Trial in Rheumatoid Arthritis with Concomitant Therapy Study Group. N Engl J Med 2000;343:1594-602.
44. Kam LY, Targan SR. TNF-alpha antagonists for the treatment of Crohn's disease. Expert Opin Pharmacother 2000;1:615-22.
45. Castell JV, Gomez-Lechon MJ, David M, Hirano T, Kishimoto T, Heinrich PC. Recombinant human interleukin-6 (IL-6/BSF-2/HSF) regulates the synthesis of acute phase proteins in human hepatocytes. FEBS Lett 1988;232:347-50.
46. Tamura T, Udagawa N, Takahashi N, et al. Soluble interleukin-6 receptor triggers osteoclast formation by interleukin 6. Proc Natl Acad Sci USA 1993;90:11924-8.
47. Yoshizaki K, Nishimoto N, Mihara M, Kishimoto T. Therapy of rheumatoid arthritis by blocking IL-6 signal transduction with a humanized anti-IL-6 receptor antibody. Springer Semin Immunopathol 1998;20:247-59.
48. Jacobsohn DA. Novel therapeutics for the treatment of graft-versus-host disease. Expert Opin Investig Drugs 2002;11:1271-80.
49. Negrusz-Kawecka, M. The role of TNF-alpha in the etiopathogenesis of heart failure. Pol Merkuriusz Lek 2002;12:69-72.
50. Katsume A, Saito H, Yamada Y, et al. Anti-interleukin 6 (IL-6) receptor antibody suppress Castleman's disease-like symptoms emerged in IL-6 transgenic mice. Cytokine 2002;21:304-11.

INFECTION AND IMMUNITY, Jan. 2008, p. 214–220 Vol. 76, No. 1
0019-9567/08/$08.00+0 doi:10.1128/IAI.01193-07

Nonpathogenic *Escherichia coli* Strain Nissle 1917 Inhibits Signal Transduction in Intestinal Epithelial Cells[▽]

Nobuhiko Kamada,[1]† Kenichi Maeda,[2]† Nagamu Inoue,[1] Tadakazu Hisamatsu,[1] Susumu Okamoto,[1] Kyong Su Hong,[2] Takaya Yamada,[3] Noriaki Watanabe,[4] Kanji Tsuchimoto,[4] Haruhiko Ogata,[1] and Toshifumi Hibi[1]*

Division of Gastroenterology and Hepatology, Department of Internal Medicine, Keio University School of Medicine, Tokyo, Japan[1]; Research Center, Research Division, JCR Pharmaceuticals Co., Ltd., Kobe, Japan[2]; Department of Experimental Animals, Center for Integrated Research in Science, Shimane University, Izumo, Japan[3]; and Department of Internal Medicine, Kitasato Institute Hospital, Tokyo, Japan[4]

Received 30 August 2007/Returned for modification 28 September 2007/Accepted 18 October 2007

Although the probiotic *Escherichia coli* strain Nissle 1917 has been used for the treatment of inflammatory bowel diseases, the precise mechanisms of action of this strain remain unclear. In the present study, we estimated the anti-inflammatory effect of *E. coli* Nissle 1917 on inflammatory responses in vitro to determine the suppressive mechanism of Nissle 1917 on the inflammatory process. To determine the effect of *E. coli* Nissle 1917, the human colonic epithelial cell line HCT15 was incubated with or without *E. coli* Nissle 1917 or another nonpathogenic *E. coli* strain, K-12, and then tumor necrosis factor alpha (TNF-α)-induced interleukin-8 (IL-8) production from HCT15 cells was assessed. Enzyme-linked immunosorbent assays and real-time quantitative PCR showed that Nissle 1917 treatment suppressed TNF-α-induced IL-8 transcription and production. In addition, results from luciferase assays indicated that Nissle 1917 inhibited IL-8 promoter activity. On the other hand, these anti-inflammatory effects were not seen with *E. coli* K-12. In addition, heat-killed Nissle 1917 or its genomic DNA did not have this anti-inflammatory effect. Surprisingly, Nissle 1917 did not affect IL-8 transactivation pathways, such as NF-κB activation, nuclear translocation, and DNA binding, or even activation of other transcriptional factors. Furthermore, it also became evident that Nissle 1917 induced the anti-inflammatory effect without contact to epithelial cells. In conclusion, these data indicate that the nonpathogenic *E. coli* strain Nissle 1917 expresses a direct anti-inflammatory activity on human epithelial cells via a secreted factor which suppresses TNF-α-induced IL-8 transactivation through mechanisms different from NF-κB inhibition.

Inflammatory bowel disease (IBD) is a disease characterized as chronic intestinal mucosal inflammation (3). In spite of recent clinical and basic research, the etiology of IBD remains unknown (16). Recent basic research has indicated that bacterial flora play an important role in the homeostasis of gut, and a dysregulated interaction between intestinal mucosa and flora may contribute to the development and the perpetuation of intestinal inflammation (22). In some genetically engineered rodent colitis models, for example, in murine lines deficient for the T-cell receptor alpha-chain gene (12), the interleukin-10 (IL-10) gene (10), or the IL-2 gene (20) and in HLA-B27 transgenic rat lines (29), the commensal bacteria are required for the development of chronic colitis. These rodent colitis models do not develop intestinal inflammation under germ-free conditions. Some clinical evidence has also indicated the contribution of intestinal flora to the development of colitis, as antibiotics are often effective in human IBD therapy (28). Furthermore, recent linkage analysis identified a single-nucleotide polymorphism of the CARD15 gene, which is the cytosolic receptor for the bacterial cell wall component muramyl dipeptide, as associated with the risk of Crohn's disease (4, 14). Thus, the regulation of the interaction between intestinal mucosa and gut flora is considered to be a novel therapeutic strategy for IBD. Probiotics are defined as living nonpathogenic organisms that confer health benefits by improving the microbial balance (23). It has been reported that probiotics have demonstrated efficacy in the treatment of human IBD (23). Nonpathogenic *Escherichia coli* strain Nissle 1917 is the active component of the microbial drug Mutaflor (Ardeypharm, Germany). This strain is used in several European countries as a probiotic drug for the treatment of IBD. Recent clinical trials have demonstrated the efficacy of Nissle 1917 for the treatment ulcerative colitis (8, 9, 18). Nissle 1917 had equivalent efficacy to mesalazine, which is commonly used for treating IBD, in the maintenance of remission of ulcerative colitis. Although several mechanisms of action have been suggested to explain the protective and anti-inflammatory effect of probiotics, the precise mechanism remains unclear. In this study, we investigated the anti-inflammatory effect of *E. coli* Nissle 1917 on proinflammatory cytokine production from intestinal epithelial cells (IECs).

* Corresponding author. Mailing address: Division of Gastroenterology and Hepatology, Department of Internal Medicine, Keio University School of Medicine, 35 Shinano-machi, Shinjuku-ku, Tokyo 160-8582, Japan. Phone and fax: 81 3 3357 6156. E-mail: thibi@sc.itc.keio.ac.jp.

† N.K. and K.M. contributed equally to this work.

▽ Published ahead of print on 29 October 2007.

MATERIALS AND METHODS

Cell culture. HCT15 cells were cultured in Dulbecco's modified Eagle's medium (DMEM) (Sigma, St. Louis, MO) supplemented with 10% heat-inactivated

fetal bovine serum (Biosource International, CA). The cells were inoculated into six-well plates (1.0×10^6 cells/well) and then incubated overnight at 37°C.

Preparation of bacteria. The *E. coli* strain Nissle 1917 (Mutaflor; DMS 6601, serotype O6:K5:H1) was kindly provided by Ardeypharm GmbH (Herdecke, Germany). Nissle 1917 and the nonpathogenic *E. coli* K-12 DH10B strain were used in this study. Bacteria were incubated in Luria-Bertani medium at 37°C in a shaker to reach mid-log phase with the density determined as 0.5 to 0.7 at A_{600}. Bacteria were collected by centrifugation, washed twice with phosphate-buffered saline (PBS), and resuspended in DMEM at up to 1.0×10^5 CFU/ml. Heat-killed bacteria were prepared by resuspending viable bacteria in PBS, followed by incubation for 30 min at 60°C. Killed bacteria were then washed with PBS and resuspended in PBS. Genomic DNA was isolated from Nissle 1917 using a Genomic DNA isolation kit (Qiagen Inc., Valencia, CA).

Treatment for *E. coli* on human IECs. The *E. coli* prepared at 1.0×10^5 CFU/ml were applied to HCT15 cells and coincubated for various lengths of time. After *E. coli* preincubation, HCT15 cells were stimulated with 20 ng/ml of tumor necrosis factor alpha (TNF-α) for 30 min without removing the bacteria. Cells were washed once with cold PBS and scraped with a cell scraper. Cells were collected and washed twice with ice-cold PBS.

ELISA) for IL-8. Collected cells were suspended in lysis buffer (0.5% NP-40, 10 mM Tris-HCl [pH 7.4], 150 mM NaCl, 1 mM EDTA, 1 mM phenylmethylsulfonyl fluoride, 10 μg/ml aprotinin, 10 μg/ml leupeptin) and left to stand on ice for 25 min. The cell lysate was centrifuged at 15,000 rpm for 5 min, and then insoluble debris was removed. The interleukin-8 (IL-8) concentration of the HCT15 cell extraction was measured by an enzyme-linked immunosorbent assay (ELISA) kit (Biosource).

Analysis of IL-8 expression by RT-PCR. HCT15 cells were incubated with live Nissle 1917 (1.0×10^5 CFU/ml), heat-killed Nissle 1917 (1.0×10^8 CFU/ml), or its genomic DNA (10 μg/ml) for 4 h and then stimulated by TNF-α. Cells were harvested after a 30-min stimulation, and total RNA was isolated using an RNeasy mini kit (Qiagen). In this process, RNA was treated with RNase-free DNase I (Qiagen) to prevent carryover of genomic DNA. The cDNA was synthesized from 2 μg of total RNA with Omniscript reverse transcriptase (Qiagen). For quantitative reverse transcription-PCR (RT-PCR), equivalent amounts of cDNAs (2 μl) and 0.5 μM concentrations of the forward and the reverse primers were used with a DyNAmo Sybr Green quantitative PCR (qPCR) kit (MJ Research, Waltham, MA). The PCRs were carried out in a thermocycler DNA Engine, Opticon2 (MJ Research). Cycling conditions for PCR amplification were 95°C for 10 min and 40 cycles of 95°C for 10 s and 58°C for 50 s. Human specific primers for IL-8 were 5′-TCTGCAGCTCTGTGTGAAGGTGCAGT T-3′ (forward) and 5′-AACCCTCTGCACCCAGTTTTCCT-3′ (reverse). β-Actin primers were 5′-CTACGTCGCCCTGGACTTCGAGC-3′ (forward) and 5′-GATGGAGCCGCCGATCCACACG-3′ (reverse).

Construction of IL-8 luciferase reporter constructs. The 5′ deletion constructs of the human IL-8 promoter corresponding to sequences from −1481 (pNAF), −130 (pN130), −112 (pN112), and −78 (pN78) to +44 bp and a promoterless plasmid (pLuc0) were kindly provided by S. Abe (Yamagata University, Japan). Site-directed mutagenesis of the IL-8 promoter was performed using a QuickChange site-directed mutagenesis kit (Stratagene). The construct containing the −130-bp sequence upstream from the transcription start site of the IL-8 gene (pN130) was used as a template plasmid. The primers used for point mutations for the activator protein 1 (AP-1) site (at −126 to −120, TGACTCA to TATC TCA; mutation is underlined) were 5′-GTGTGATATCTCAGGTTTGCCCTG AGGG-3′ (forward) and 5′-CCCTCAGGGCAAACCTGAGATATCACAC-3′ (reverse). For C/EBPβ (point mutations at −94 to −81, CAGTTGCAAATCGT to AGCTTGCAAATCGT), the primers were 5′-GGATGGGCCATAGCTTG CAAATCGTGG-3′ (forward) and 5′-CCACGATTTGCAAGCTATGGCCCA TCC-3′ (reverse). For NF-κB (point mutations at −80 to −71, GGAATTTCCT to TAACTTTCCT), the primers were 5′-GTTGCAAATCGTTAACTTTCCTC TGACATAATG3′ (forward) and 5′-CATTATGTCAGAGGAAAGTTAACG ATTTGCAAC-3′ (reverse). These plasmid constructs were confirmed by sequencing.

DNA transfection and luciferase reporter assay. A total of 1×10^6 HCT15 cells/well were seeded on six-well plates. After 24 h, the cells were transiently transfected with the indicated reporter plasmid (1 μg/well) with the *Renilla* luciferase expression plasmid pRL-TK (0.1 μg/ml) (Promega), using FuGENE 6 transfection reagent (Roche). After incubation of 24 h, cells were washed twice with PBS and cultured for 4 h in serum and antibiotic-free Hank's balanced buffered salt containing calcium chloride with or without Nissle 1917 (1.0×10^7 CFU/ml). Cells were then stimulated by TNF-α (20 ng/ml) for 30 min. The luciferase activity of total cell lysates was measured using a dual luciferase reporter assay system (Promega). The *Renilla* luciferase reporter gene pRL-TK was used as an internal control.

Western blot analysis. HCT15 cells were grown in six-well plates. The cells were pretreated with 1.0×10^5 CFU/ml Nissle 1917 for 4 h and then stimulated with 20 ng/ml of TNF-α. Total cell lysates and nuclear protein from HCT15 cells were obtained using mammalian protein extraction reagent and a nuclear and cytosol protein extraction kit (Pierce). Each protein was fractionated by sodium dodecyl sulfate-polyacrylamide gel electrophoresis and transferred onto polyvinylidene difluoride membranes (Millipore). Membranes were blocked with 5% milk and incubated overnight with anti-p65 polyclonal antibody (Santa Cruz), anti-IκBα polyclonal antibody (Santa Cruz), or anti-β-actin polyclonal antibody (Sigma) at 4°C, followed by incubation at room temperature for 1 h with horseradish peroxidase-linked anti-rabbit antibody (Cell Signaling). Staining was detected using ECL Western blotting detection reagent (Amersham Biosciences).

Nuclear protein extraction and electrophoretic mobility shift assay (EMSA). Nuclear extracts were prepared from HCT15 cells using a nuclear and cytosol protein extraction kit (Pierce). Both double-stranded oligonucleotide probes corresponding to the wild-type NF-κB binding site (5′-AGTTGAGGGGACTT TCCCAGGC-3′ and 3′-TCAACTCCCCTGAAAGGGTCCG-5′ [Promega]) and the mutated NF-κB binding site (5′-AGTTGAGGCGACTTTCCCAGG C-3′ and 3′-TCAACTCCGCTGAAAGGGTCCG-5′; mutations are underlined [Santa Cruz]) were used as probes or cold competitors to analyze the interaction between NF-κB and DNA. The probes were labeled with [γ-^{32}P]ATP (3,000 Ci/mmol at 10 mCi/ml) (Amersham Biosciences) using T4 polynucleotide kinase (Promega) and purified by MicroSpin G-25 columns (Amersham Biosciences). The binding reaction was performed using a gel shift assay system (Promega) and 20 μg of nuclear extract. For the competition assay, a 100-fold excess of unlabeled oligonucleotide was added to the reaction mixture. Samples were electrophoresed by a 4% nondenaturing acrylamide gel in 0.5× Tris-borate-EDTA buffer at 150 V for 1.5 h. The gel was placed on a filter paper and dried with a Gel Dryer (Bio-Rad) for 1 h. Then, the gel was exposed to a phosphorimaging plate overnight and analyzed by BAS 2000 systems.

ChIP assay. The HCT15 cells were cross-linked by 1% formaldehyde for 15 min at 37°C. Cross-linking was stopped by the addition of 0.125 M glycine, and cells were incubated for 10 min at 4°C and then washed twice with ice-cold PBS. Following cross-linking, the cells were collected and resuspended in sodium dodecyl sulfate lysis buffer (Upstate) containing protease inhibitors (1 mM phenylmethylsulfonyl fluoride, 1 μg/ml aprotinin, and 1 μg/ml leupeptin), and the chromatin was cleaved into 500- to 1,000-bp fragments by sonication. Samples were then diluted with chromatin immunoprecipitation (ChIP) dilute buffer and incubated overnight with 3 μg of specific antibodies for p65 (Upstate) or RNA polymerase II (Santa Cruz), followed by incubation with protein A-agarose saturated with bovine serum albumin and salmon sperm DNA. Agarose-bound immune complexes were collected, washed, and eluted. The protein-DNA cross-links were incubated overnight at 65°C to reverse cross-links. After proteinase K digestion, DNA was purified using a PCR purification kit (Qiagen). Purified immunoprecipitated chromatin and input samples were analyzed by real-time qPCR using a DyNAmo Sybr Green qPCR kit and the thermocycler DNA Engine Opticon2 (MJ Research). Primer pairs for monitoring the IL-8 promoter region were 5′GGGCCATCAGTTGCAAATC-3′ (forward) and 5′-TTCCTTCCGGTGGTTTCTTC-3′ (reverse). Cycling conditions for PCR amplification were 95°C for 10 min and 40 cycles of 95°C for 10 s and 58°C for 50 s.

Analysis of the suppressive effect of Nissle 1917 secreted factor. HCT15 cells were cultured in the lower well of the Transwell filter membrane system (0.4-μm pore size; Costar). *E. coli* Nissle 1917 or K-12 DH10B prepared at 1.0×10^5 CFU/ml was applied to the upper well and coincubated for 4 h. After preincubation, cells were stimulated with 20 ng/ml of TNF-α for 30 min. In a separate test, Nissle 1917 or K-12 DH10B (1.0×10^5 CFU/ml) alone was incubated in DMEM for 4 h, and then supernatants were separated by passage through 0.22-μm-pore-size filters. Filtered culture supernatants were then applied to the HCT15 cells and incubated for 30 min. After incubation, cells were stimulated with 20 ng/ml of TNF-α for 30 min. For both culture methods, after stimulation with TNF-α, cells were washed once with cold PBS and scraped with a cell scraper. Cells were then collected and washed twice with ice-cold PBS. Cellular proteins were extracted by the protein extraction method, described above, and IL-8 concentrations were measured by ELISA.

Statistical analysis. Statistical analysis was performed using GraphPad Prism software, version 4.0 (San Diego, CA). Differences at a P value of <0.05 were considered to be significant. All data are expressed as means ± standard error of the mean (SEM).

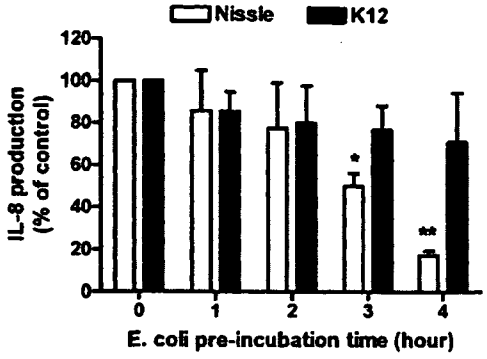

FIG. 1. *E. coli* Nissle 1917 suppresses TNF-α-induced IL-8 production. HCT15 cells were pretreated for various lengths of time with 1×10^5 CFU/ml nonpathogenic *E. coli* strain Nissle 1917 or K-12 DH10B and were then stimulated with 20 ng/ml TNF-α for 30 min. After stimulation, intracellular proteins were extracted, and IL-8 protein amounts were determined by ELISA. Data are expressed as the percentage of IL-8 production in HCT15 cells stimulated with TNF-α without Nissle 1917 treatment (defined as 100%) and are given as means ± SEM of three to four experiments. Significance was determined by comparison with the values of TNF-α-induced IL-8 in the *E. coli* untreated group (Dunnett's test). *, $P < 0.05$; **, $P < 0.01$.

RESULTS

***E. coli* Nissle 1917 inhibited TNF-α-induced IL-8 production by IECs.** To determine the effect of Nissle 1917, human IEC line HCT15 cells were untreated or pretreated with *E. coli* Nissle 1917 and another nonpathogenic *E. coli* strain, K-12 DH10B (1×10^5 CFU/ml), for 1 to 4 h, followed by stimulation with TNF-α (20 ng/ml) for 30 min. After stimulation, the intracellular protein levels of the proinflammatory chemokine IL-8 were assayed by ELISA. The basal production of IL-8 was not affected by *E. coli* Nissle 1917 and K-12; however, TNF-α-induced IL-8 production was significantly inhibited by a 3- to 4-h pretreatment with Nissle 1917 but not by K-12 (Fig. 1). Another enteric *E. coli* strain, ATCC 25922, did not show the inhibitory effect on TNF-α-induced IL-8 production, similar to K-12 (data not shown). These results suggest that only the probiotic strain Nissle 1917 has an anti-inflammatory effect among the nonpathogenic *E. coli* strains. Next, we examined the effect of Nissle 1917 on IL-8 mRNA expression after TNF-α stimulation using real-time qPCR. Consistent with the result of protein production, TNF-α-induced IL-8 mRNA transcription was also suppressed by pretreatment with *E. coli* Nissle 1917 (Fig. 2A) but not by *E. coli* K-12 (data not shown). Moreover, the proinflammatory chemokine methyl-accepting chemotaxis protein 1, which was strongly induced by TNF-α, was also suppressed by Nissle 1917 (data not shown). Because recent studies have reported that genomic DNA itself has anti-inflammatory effects in vitro and in vivo (5, 7, 17), we investigated the effect of genomic DNA from Nissle 1917 and heat-killed Nissle 1917 on IL-8 production from TNF-α-treated HCT15 cells. As shown in Fig. 2B, heat-killed Nissle 1917 and its genomic DNA did not show such an anti-inflammatory effect. These results indicated that only the live *E. coli* Nissle 1917, and not heat-killed and genomic DNA alone, can inhibit TNF-α-induced IL-8 production, even in the transcriptional process.

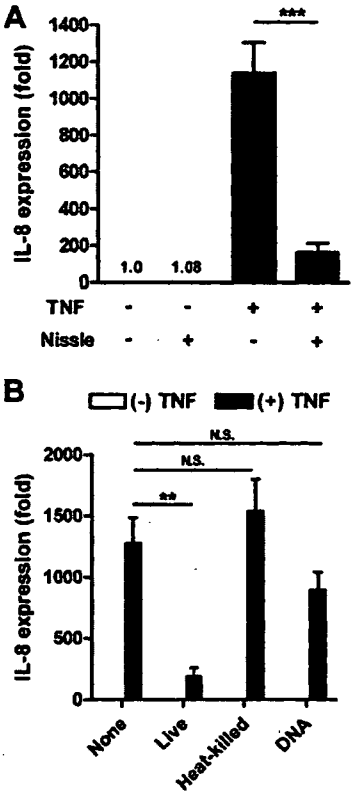

FIG. 2. *E. coli* Nissle 1917 suppresses TNF-α-triggered transcription of IL-8 via its viable form. (A) HCT15 cells were pretreated with Nissle 1917 (1×10^5 CFU/ml) for 4 h and then stimulated with 20 ng/ml TNF-α. After stimulation for 30 min, IL-8 mRNA expression was analyzed by real-time RT-PCR. (B) HCT15 cells were pretreated with living Nissle 1917 bacteria (1×10^5 CFU/ml), heat-killed Nissle 1917 (1×10^8 CFU/ml), or its genomic DNA (10 μg/ml) for 4 h and then stimulated by 20 ng/ml TNF-α for 30 min. IL-8 mRNA expression was analyzed by real-time RT-PCR. Data are shown as relative expression against β-actin mRNA and given as means ± SEM of five independent experiments. Significance was determined by comparison with the values of TNF-α-induced IL-8 in the *E. coli* untreated group (Sheffe's test). **, $P < 0.01$; ***, $P < 0.001$.

***E. coli* Nissle 1917 suppresses the promoter activity of human IL-8.** To identify the transcriptional regulation of IL-8 by Nissle 1917, a series of luciferase reporter plasmids of the IL-8 promoter were used. As shown in Fig. 3A, luciferase activity in HCT15 cells transfected with a vector containing the entire 1,481-bp upstream DNA fragment (pNAF1481) was higher than that obtained with the empty pLuc0 vector by TNF-α stimulation. Promoter activity was significantly decreased in pN78 compared with pN112. This result indicated that the sequence upstream of −78 is required for TNF-α-induced IL-8 promoter activity. Consistent with the results of real-time PCR and ELISA, Nissle 1917 pretreatment suppressed the TNF-α-induced transactivation of IL-8 promoter activity in both pN130 and the deletion mutant of the AP-1 binding sequence, pN112. This result suggests that AP-1 is not the crucial target for the suppressive effect of Nissle 1917 on TNF-α-induced IL-8 transactivation. In addition, the nonpathogenic *E. coli* strain K-12 did not inhibit IL-8 promoter activity in either ELISA or RT-PCR analysis (data not shown). To identify the

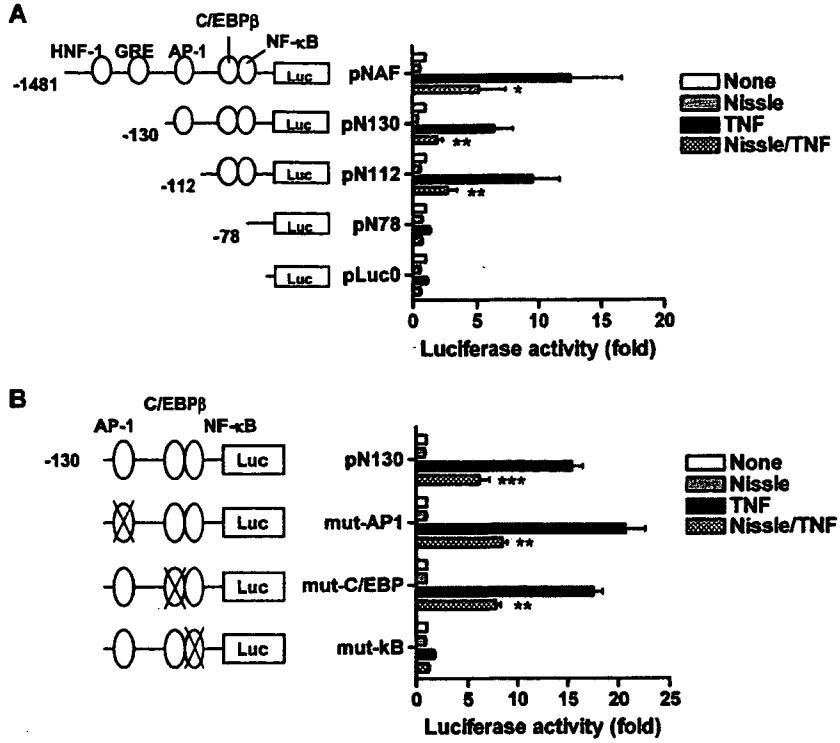

FIG. 3. Nissle 1917 inhibits IL-8 promoter activity. (A) HCT15 cells were transfected with 5′ deletions of the IL-8 promoter-driven luciferase. Each sample contained *Renilla* luciferase vector DNA (pRL-TK) for normalization of transfection efficiency. Twenty-four hours after transfection, cells were treated with Nissle 1917 bacteria (1.0×10^7 CFU/ml) for 4 h in serum-free Hank's balanced salt solution and then stimulated with TNF-α for 30 min. Cells were lysed and assayed for luciferase activity. (B) The proximal human IL-8 promoter region (position −130) was used for mutation assays. Mutant (mut) vectors of NF-κB, C/EBPβ, or AP-1 binding sites were transfected into HCT15 cells and then treated with Nissle 1917 and TNF-α, as described above. Cells were lysed and assayed for luciferase activity. The results are presented as the relative increase in activation (*n*-fold) of control cells and are given as means ± SEM of four to six independent experiments. Significance was determined by comparison with the values of TNF-α-induced IL-8 in the *E. coli* untreated group (paired Student's *t* test). *, $P < 0.05$; **, $P < 0.01$; ***, $P < 0.001$. GRE, glucocorticoid response element.

responsible element of the IL-8 promoter sequence in the Nissle 1917-mediated inhibition, mutated constructs of each transcription factor binding sequence were generated (Fig. 3B). As a result of the deletion study, a mutated construct in the AP-1 binding site showed increased luciferase activity as a result of TNF-α stimulation and the inhibitory effects of Nissle 1917. Moreover, the construct with a mutation of the C/EBPβ (CCAAT/enhancer-binding protein β) binding site also had a normal response to TNF-α stimulation and decreased luciferase activity with Nissle 1917 pretreatment. These results suggest that AP-1 and C/EBPβ were not responsible for the suppressive effect of Nissle 1917. However, up-regulation of luciferase activity by TNF-α stimulation was completely suppressed by mutation of the NF-κB binding site, as indicated by the results of the deletion study.

To investigate whether Nissle 1917 can inhibit NF-κB activation, which is considered the element responsible for the augmentation of IL-8 transcription by TNF-α, we next analyzed the activation of NF-κB by Western blot analysis. In the normal state, NF-κB exists in the cytoplasm as a nonactivated complex consisting of three subunits: a transactivating subunit p65 (also called RelA), p50, and an inhibitory subunit, IκBα. With exposure to an inflammatory stimulus such as TNF-α, the inhibitory subunit IκBα is phosphorylated and degraded; then the transactivating subunit p65-p50 heterodimer is translocated into the nucleus. As shown in Fig. 4A and B, IκBα degradation and nuclear translocation of the p65 subunit were observed after TNF-α stimulation. However, treatment with Nissle 1917 did not suppress these processes. These data indicate that Nissle 1917 does not affect the nuclear translocation of p65. To determine whether Nissle 1917 prevented the DNA binding process of transcriptional factors, we carried out EMSAs. As shown in Fig. 4C, TNF-α stimulation increased DNA binding of NF-κB, but this was not inhibited by Nissle 1917 treatment (lanes 3 and 4). Another transcriptional factor, C/EBPβ, did not prevent DNA binding with Nissle 1917 treatment (data not shown). Since EMSAs assessed the binding of NF-κB consensus motifs in vitro, p65 recruitment to the endogenous IL-8 promoter in intact cells was tested by ChIP assay. Stimulation of TNF-α caused extensive recruitment of the p65 NF-κB subunit and transcriptional cofactor CBP to the IL-8 promoter, and this was not blocked by Nissle 1917 treatment (Fig. 4D). Thus, the suppressive effect of Nissle 1917 on the transcription of TNF-α-induced IL-8 is independent of the NF-κB activation process.

Nissle 1917 secreted factor suppressed TNF-a induced IL-8 production. To determine the anti-inflammatory effect of Nissle 1917 secreted factors, we used the Transwell system

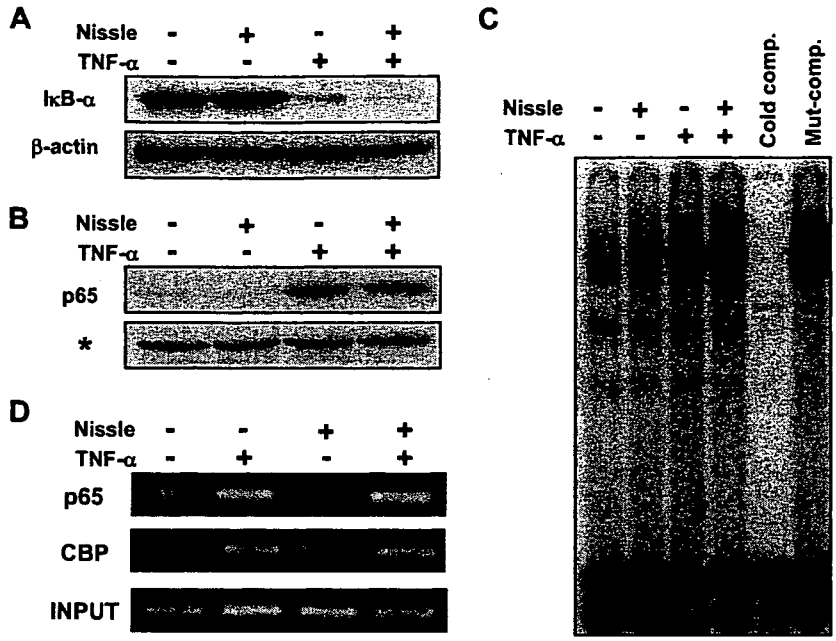

FIG. 4. Nissle 1917 does not affect NF-κB transactivation pathways. (A) HCT15 cells were pretreated with Nissle 1917 bacteria (1×10^5 CFU/ml) for 4 h and then stimulated with 20 ng/ml TNF-α. After stimulation for 30 min, whole cellular proteins were extracted and used for Western blotting of IκBα and β-actin. (B) HCT15 cells were treated with Nissle 1917 and TNF-α as before, and then nuclear proteins were extracted. Extracted nuclear proteins were used for NF-κB p65 Western blotting. A nonspecific protein recognized by the antibody was used as loading control (asterisk). Data are representative of one of three independent experiments. (C) HCT15 cells were pretreated with Nissle 1917 bacteria (1×10^5 CFU/ml) for 4 h and then stimulated with 20 ng/ml TNF-α. After stimulation for 30 min, nuclear proteins were extracted. EMSAs were performed with a ^{32}P-labeled probe containing the NF-κB binding site and nuclear extracts from TNF-α-stimulated HCT15 cells with or without Nissle 1917 pretreatment. Data are representative of one of three independent experiments. (D) HCT15 cells were pretreated with Nissle 1917 bacteria (1×10^5 CFU/ml) for 4 h and then stimulated with 20 ng/ml TNF-α for 30 min. ChIP assays were performed with the indicated antibodies. The detection of the immunoprecipitated human IL-8 promoter was analyzed by PCR with promoter-specific primers. Data are representative of one of three independent experiments. Mut, mutant; comp, competitor.

(Fig. 5A) and *E. coli* culture supernatant (Fig. 5B) in tandem with control strain K-12 for the IL-8 prevention assay. Interestingly, Nissle 1917 inhibited TNF-α-induced IL-8 production but not through contact with the cells. These results suggest that a currently unknown Nissle 1917 secreted factor in the culture supernatant suppressed the TNF-α-triggered inflammatory processes.

DISCUSSION

IECs play a role as a barrier both functionally and structurally. IECs separate the host's internal milieu from the external environment. In addition to the barrier function, it has become evident recently that IECs play an important role in maintaining homeostasis. IECs produce antimicrobial peptides, such as defensins, and protect the host from attachment of luminal bacteria (21, 30). Moreover, in addition to a direct bactericidal role, IEC-derived factors can promote an anti-inflammatory type of dendritic cells and macrophages differentiation to induce mucosal tolerances against luminal bacteria (19, 26). Furthermore, IECs can produce several chemokines and proinflammatory cytokines to induce the migration of granulocytes, lymphocytes, and dendritic cells, resulting in the induction of host immunity (1). Previous studies have demonstrated that IECs produce IL-8 in response to several pathogenic bacteria (6). Thus, IECs function as a defensive frontline of host mucosal immunity. Although the therapeutic mechanism of action

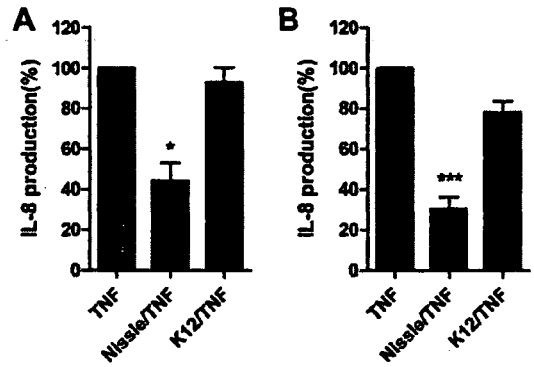

FIG. 5. Nissle 1917 inhibited TNF-α-induced IL-8 production without adherence of bacteria to the epithelial cells. (A) HCT15 cells were cultured in the lower well of a Transwell filter membrane system (0.4-μm pore size). *E. coli* Nissle 1917 or K-12 DH10B prepared at 1.0×10^5 CFU/ml was applied to the upper well and coincubated for 4 h. After preincubation, cells were stimulated with 20 ng/ml of TNF-α for 30 min. (B) *E. coli* Nissle 1917 or K-12 DH10B (1.0×10^5 CFU/ml) alone was incubated in DMEM for 4 h, and then supernatants were separated by passage through a 0.22-μm-pore-size filter. Filtered culture supernatants were then applied to the HCT15 cells and incubated for 30 min. After incubation, cells were stimulated with 20 ng/ml of TNF-α for 30 min. After stimulation, intracellular proteins were extracted, and IL-8 protein amounts were determined by ELISA. Data are expressed as the percentage of IL-8 production in *E. coli* untreated controls (defined as 100%). Data are given as means ± SEM of the at least three experiments. *, $P < 0.05$; ***, $P < 0.001$ (Dunnett's test).

of probiotics in IBD remains unclear, it was previously reported that some nonpathogenic resident bacteria and probiotic bacteria strains suppress IL-8 production from IECs. For example, nonpathogenic *Salmonella enterica* serovar Typhimurium (13), *Lactobacillus reuteri* (11), or the probiotic VSL#3 (5) prevented TNF-α-induced IL-8 production. These suppressive functions of nonpathogenic resident bacteria and probiotic strains may contribute to maintaining intestinal homeostasis or show therapeutic effects as a probiotics. Consistent with studies of other probiotic bacteria, we found a suppressive effect of nonpathogenic *E. coli* Nissle 1917 on TNF-α-induced IL-8 production. This function is one of the therapeutic mechanisms of Nissle 1917 on IBD. There have been some reports on the inhibitory mechanisms of the signal transduction pathway by probiotic bacteria: a nonpathogenic *Salmonella* species was found to inhibit IκB ubiquitination and the subsequent NF-κB activation (13); *L. reuteri* inhibited IκB degradation (11); VSL#3 suppressed the NF-κB activation pathway through proteosome inhibition (15); and genomic DNA from VSL#3 inhibited the phosphorylation of p38 mitogen-activated protein kinase (5). In our present study, Nissle 1917 did not inhibit any of the signal transduction pathways described above, although mRNA transcription of IL-8 was suppressed. In fact, IκB degradation, NF-κB p65 nuclear translocation, and DNA binding were not dramatically altered even after Nissle 1917 treatment. These results indicated that Nissle 1917 does not suppress the NF-κB activation pathway, in contrast to *L. reuteri*. Moreover, our study demonstrated that Nissle 1917 does not affect another signal transduction pathway for IL-8 expression, namely, activation of C/EBPβ and phosphorylation of p38 mitogen-activated protein kinase (data not shown). Therefore, how does Nissle 1917 prevent IL-8 transcription if not through the inhibition of NF-κB or activation of other transcriptional factors? There is a possibility that Nissle 1917 may suppress the post-DNA binding process of transcriptional factors, prevent activation of basic transcriptional factors or RNA polymerase, or suppress chromatin remodeling processes, such as phosphorylation or acetylation of histones.

What is the active component of probiotic bacteria that is responsible for their anti-inflammatory function? Ma et al. demonstrated that *L. reuteri* inhibited TNF-α-induced IL-8 expression only through the viable form (11), and Petrof et al. reported that the VSL#3 secreted factor prevented NF-κB activation (15). In contrast, it was also demonstrated by Jijon et al. and Rachmilewitz et al. that VSL#3 genomic DNA had an anti-inflammatory function in vitro and in vivo (5, 17). We have already demonstrated that Nissle 1917 heat-killed antigen and its genomic DNA can prevent murine colitis (7). However, in our present data, heat-killed Nissle 1917 or its DNA could not suppress the TNF-α-induced IL-8 expression from IECs. This suppressive effect on the production of IL-8 from IECs was displayed only by live Nissle 1917 bacteria. Recently, the therapeutic mechanisms of Nissle 1917 have been proposed based on results from in vitro experiments. For example, Nissle 1917 increased the expression of antibacterial peptides, human β-defensins, by epithelial cell lines through the NF-κB and AP-1 pathways (24, 31); Nissle 1917 modulated T-cell cycling and expansion via Toll-like receptor 2 (TLR2) signaling (27). In addition, an anti-inflammatory effect of Nissle 1917 was reported by some investigators using in vivo experiments in several models of murine experimental colitis. We along with other groups have reported that Nissle 1917 treatment prevented both acute and chronic colitis via suppression of the production of proinflammatory cytokines by mesenteric lymph nodes or lamina propria mononuclear cells (7, 25). Moreover, Grabig et al. reported that Nissle 1917 ameliorated acute dextran sodium sulfate-induced colitis via a TLR2- and TLR4-dependent pathway (2). In the present study, we have demonstrated the first direct evidence of the anti-inflammatory effect of Nissle 1917. The findings presented here could support the anti-inflammatory effect of Nissle 1917 in murine and human intestinal inflammation.

In conclusion, we have provided evidence that the probiotic *E. coli* strain Nissle 1917 as well as other probiotic strains suppresses TNF-α-induced IL-8 secretion from IECs. Moreover, the mechanism by which Nissle 1917 suppresses IL-8 might be independent of the inhibition of the NF-κB signaling pathway. Thus, our findings may provide new insight into the mechanisms of action of the probiotic strain Nissle 1917 in IBD.

ACKNOWLEDGMENTS

We thank A. Abe for helpful advice and S. Abe for providing us with IL-8 promoter products.

This work was supported in part by grants from JCR Pharmaceuticals Co., Ltd. (Kobe, Japan).

REFERENCES

1. **Dahan, S., F. Roth-Walter, P. Arnaboldi, S. Agarwal, and L. Mayer.** 2007. Epithelia: lymphocyte interactions in the gut. Immunol. Rev. 215:243–253.
2. **Grabig, A., D. Paclik, C. Guzy, A. Dankof, D. C. Baumgart, J. Erckenbrecht, B. Raupach, U. Sonnenborn, J. Eckert, R. R. Schumann, B. Wiedenmann, A. U. Dignass, and A. Sturm.** 2006. *Escherichia coli* strain Nissle 1917 ameliorates experimental colitis via Toll-like receptor 2- and Toll-like receptor 4-dependent pathways. Infect. Immun. 74:4075–4082.
3. **Hibi, T., and H. Ogata.** 2006. Novel pathophysiological concepts of inflammatory bowel disease. J. Gastroenterol. 41:10–16.
4. **Hugot, J. P., M. Chamaillard, H. Zouali, S. Lesage, J. P. Cezard, J. Belaiche, S. Almer, C. Tysk, C. A. O'Morain, M. Gassull, V. Binder, Y. Finkel, A. Cortot, R. Modigliani, P. Laurent-Puig, C. Gower-Rousseau, J. Macry, J. F. Colombel, M. Sahbatou, and G. Thomas.** 2001. Association of NOD2 leucine-rich repeat variants with susceptibility to Crohn's disease. Nature 411:599–603.
5. **Jijon, H., J. Backer, H. Diaz, H. Yeung, D. Thiel, C. McKaigney, C. De Simone, and K. Madsen.** 2004. DNA from probiotic bacteria modulates murine and human epithelial and immune function. Gastroenterology 126: 1358–1373.
6. **Jung, H. C., L. Eckmann, S. K. Yang, A. Panja, J. Fierer, E. Morzycka-Wroblewska, and M. F. Kagnoff.** 1995. A distinct array of proinflammatory cytokines is expressed in human colon epithelial cells in response to bacterial invasion. J. Clin. Investig. 95:55–65.
7. **Kamada, N., N. Inoue, T. Hisamatsu, S. Okamoto, K. Matsuoka, T. Sato, H. Chinen, K. S. Hong, T. Yamada, Y. Suzuki, T. Suzuki, N. Watanabe, K. Tsuchimoto, and T. Hibi.** 2005. Nonpathogenic *Escherichia coli* strain Nissle 1917 prevents murine acute and chronic colitis. Inflamm. Bowel Dis. 11:455–463.
8. **Kruis, W., P. Fric, J. Pokrotnieks, M. Lukas, B. Fixa, M. Kascak, M. A. Kamm, J. Weismueller, C. Beglinger, M. Stolte, C. Wolff, and J. Schulze.** 2004. Maintaining remission of ulcerative colitis with the probiotic *Escherichia coli* Nissle 1917 is as effective as with standard mesalazine. Gut 53: 1617–1623.
9. **Kruis, W., E. Schutz, P. Fric, B. Fixa, G. Judmaier, and M. Stolte.** 1997. Double-blind comparison of an oral *Escherichia coli* preparation and mesalazine in maintaining remission of ulcerative colitis. Aliment Pharmacol. Ther. 11:853–858.
10. **Kühn, R., J. Lohler, D. Rennick, K. Rajewsky, and W. Muller.** 1993. Interleukin-10-deficient mice develop chronic enterocolitis. Cell 75:263–274.
11. **Ma, D., P. Forsythe, and J. Bienenstock.** 2004. Live *Lactobacillus reuteri* is essential for the inhibitory effect on tumor necrosis factor alpha-induced interleukin-8 expression. Infect. Immun. 72:5308–5314.
12. **Mombaerts, P., E. Mizoguchi, M. J. Grusby, L. H. Glimcher, A. K. Bhan, and**

S. Tonegawa. 1993. Spontaneous development of inflammatory bowel disease in T cell receptor mutant mice. Cell 75:274–282.
13. Neish, A. S., A. T. Gewirtz, H. Zeng, A. N. Young, M. E. Hobert, V. Karmali, A. S. Rao, and J. L. Madara. 2000. Prokaryotic regulation of epithelial responses by inhibition of IκB-α ubiquitination. Science 289:1560–1563.
14. Ogura, Y., D. K. Bonen, N. Inohara, D. L. Nicolae, F. F. Chen, R. Ramos, H. Britton, T. Moran, R. Karaliuskas, R. H. Duerr, J. P. Achkar, S. R. Brant, T. M. Bayless, B. S. Kirschner, S. B. Hanauer, G. Nunez, and J. H. Cho. 2001. A frameshift mutation in NOD2 associated with susceptibility to Crohn's disease. Nature 411:603–606.
15. Petrof, E. O., K. Kojima, M. J. Ropeleski, M. W. Musch, Y. Tao, C. De Simone, and E. B. Chang. 2004. Probiotics inhibit nuclear factor-κB and induce heat shock proteins in colonic epithelial cells through proteasome inhibition. Gastroenterology 127:1474–1487.
16. Podolsky, D. K. 2002. Inflammatory bowel disease. N. Engl. J. Med. 347: 417–429.
17. Rachmilewitz, D., K. Katakura, F. Karmeli, T. Hayashi, C. Reinus, B. Rudensky, S. Akira, K. Takeda, J. Lee, K. Takabayashi, and E. Raz. 2004. Toll-like receptor 9 signaling mediates the anti-inflammatory effects of probiotics in murine experimental colitis. Gastroenterology 126:520–528.
18. Rembacken, B. J., A. M. Snelling, P. M. Hawkey, D. M. Chalmers, and A. T. Axon. 1999. Non-pathogenic *Escherichia coli* versus mesalazine for the treatment of ulcerative colitis: a randomised trial. Lancet 354:635–639.
19. Rimoldi, M., M. Chieppa, V. Salucci, F. Avogadri, A. Sonzogni, G. M. Sampietro, A. Nespoli, G. Viale, P. Allavena, and M. Rescigno. 2005. Intestinal immune homeostasis is regulated by the crosstalk between epithelial cells and dendritic cells. Nat. Immunol. 6:507–514.
20. Sadlack, B., H. Merz, H. Schorle, A. Schimpl, A. C. Feller, and I. Horak. 1993. Ulcerative colitis-like disease in mice with a disrupted interleukin-2 gene. Cell 75:253–261.
21. Salzman, N. H., M. A. Underwood, and C. L. Bevins. 2007. Paneth cells, defensins, and the commensal microbiota: a hypothesis on intimate interplay at the intestinal mucosa. Semin. Immunol. 19:70–83.
22. Sartor, R. B. 2006. Mechanisms of disease: pathogenesis of Crohn's disease and ulcerative colitis. Nat. Clin. Pract. Gastroenterol. Hepatol. 3:390–407.
23. Sartor, R. B. 2004. Therapeutic manipulation of the enteric microflora in inflammatory bowel diseases: antibiotics, probiotics, and prebiotics. Gastroenterology 126:1620–1633.
24. Schlee, M., J. Wehkamp, A. Altenhoefer, T. A. Oelschlaeger, E. F. Stange, and K. Fellermann. 2007. Induction of human beta-defensin 2 by the probiotic *Escherichia coli* Nissle 1917 is mediated through flagellin. Infect. Immun. 75:2399–2407.
25. Schultz, M., U. G. Strauch, H. J. Linde, S. Watzl, F. Obermeier, C. Gottl, N. Dunger, N. Grunwald, J. Scholmerich, and H. C. Rath. 2004. Preventive effects of *Escherichia coli* strain Nissle 1917 on acute and chronic intestinal inflammation in two different murine models of colitis. Clin. Diagn. Lab Immunol. 11:372–378.
26. Spöttl, T., M. Hausmann, M. Kreutz, A. Peuker, D. Vogl, J. Scholmerich, W. Falk, R. Andreesen, T. Andus, H. Herfarth, and G. Rogler. 2001. Monocyte differentiation in intestine-like macrophage phenotype induced by epithelial cells. J. Leukoc. Biol. 70:241–251.
27. Sturm, A., K. Rilling, D. C. Baumgart, K. Gargas, T. Abou-Ghazale, B. Raupach, J. Eckert, R. R. Schumann, C. Enders, U. Sonnenborn, B. Wiedenmann, and A. U. Dignass. 2005. *Escherichia coli* Nissle 1917 distinctively modulates T-cell cycling and expansion via toll-like receptor 2 signaling. Infect. Immun. 73:1452–1465.
28. Sutherland, L., J. Singleton, J. Sessions, S. Hanauer, E. Krawitt, G. Rankin, R. Summers, H. Mekhjian, N. Greenberger, M. Kelly, et al. 1991. Double blind, placebo controlled trial of metronidazole in Crohn's disease. Gut 32:1071–1075.
29. Taurog, J. D., S. D. Maika, W. A. Simmons, M. Breban, and R. E. Hammer. 1993. Susceptibility to inflammatory disease in HLA-B27 transgenic rat lines correlates with the level of B27 expression. J. Immunol. 150:4168–4178.
30. Wehkamp, J., K. Fellermann, K. R. Herrlinger, C. L. Bevins, and E. F. Stange. 2005. Mechanisms of disease: defensins in gastrointestinal diseases. Nat. Clin. Pract. Gastroenterol. Hepatol. 2:406–415.
31. Wehkamp, J., J. Harder, K. Wehkamp, B. Wehkamp-von Meissner, M. Schlee, C. Enders, U. Sonnenborn, S. Nuding, S. Bengmark, K. Fellermann, J. M. Schroder, and E. F. Stange. 2004. NF-κB- and AP-1-mediated induction of human beta defensin-2 in intestinal epithelial cells by *Escherichia coli* Nissle 1917: a novel effect of a probiotic bacterium. Infect. Immun. 72:5750–5758.

Editor: R. P. Morrison

GASTROENTEROLOGY 2008;134:481–490

Exacerbating Role of γδ T Cells in Chronic Colitis of T-Cell Receptor α Mutant Mice

MASANOBU NANNO,[*] YASUYOSHI KANARI,[‡] TOMOAKI NAITO,[§,‖] NAGAMU INOUE,[¶] TADAKAZU HISAMATSU,[¶] HIROSHI CHINEN,[¶] KEN SUGIMOTO,[#,**] YASUYO SHIMOMURA,[#,**] HIDEO YAMAGISHI,[‡] TETSUO SHIOHARA,[‡‡] SATOSHI UEHA,[§§] KOUJI MATSUSHIMA,[§§] MAKOTO SUEMATSU,[‖] ATSUSHI MIZOGUCHI,[#,**] TOSHIFUMI HIBI,[¶] ATUL K. BHAN,[#,**] and HIROMICHI ISHIKAWA[§]

*Yakult Central Institute for Microbiological Research, Tokyo; ‡Department of Biophysics, Graduate School of Science, Kyoto University, Kyoto; §Department of Microbiology and Immunology, Keio University School of Medicine, Tokyo; ‖Department of Biochemistry and Integrative Medical Biology, Keio University School of Medicine, Tokyo; ¶Department of Internal Medicine, Keio University School of Medicine, Tokyo, Japan; #Center for the Study of Inflammatory Bowel Disease, Massachusetts General Hospital, Boston; **Department of Pathology, Massachusetts General Hospital, Boston, Massachusetts; ‡‡Department of Dermatology, Kyorin University School of Medicine, Tokyo, Japan; and §§Department of Molecular Preventive Medicine, Graduate School of Medicine, University of Tokyo, Tokyo, Japan*

Background & Aims: **T-cell receptor (TCR) γδ T cells are an important component of the mucosal immune system and regulate intestinal epithelial homeostasis. Interestingly, there is a significant increase in γδ T cells in the inflamed mucosa of patients with ulcerative colitis (UC). However, the role of γδ T cells in chronic colitis has not been fully identified.** ***Methods:*** **TCRα-deficient mice, which spontaneously develop chronic colitis with many features of human UC including an increase in γδ T-cell population, represent an excellent model to investigate the role of γδ T cells in UC-like colitis. To identify the role of γδ T cells in this colitis, we herein have generated TCRγ-deficient mice through deletion of all TCR Cγ genes (Cγ1, Cγ2, Cγ3, and Cγ4) using the Cre/*loxP* site-specific recombination system and subsequently crossing these mice with TCRα-deficient mice.** ***Results:*** **An increase in colonic γδ T cells was associated with the development of human UC as well as UC-like disease seen in TCRα-deficient mice. Interestingly, the newly established TCRα$^{-/-}$ × TCRγ$^{-/-}$ double mutant mice developed significantly less severe colitis as compared with TCRα-deficient mice. The suppression of colitis in TCRα$^{-/-}$ × TCRγ$^{-/-}$ double mutant mice was associated with a significant reduction of proinflammatory cytokine and chemokine productions and a decrease in neutrophil infiltration.** ***Conclusions:*** **γδ T cells are involved in the exacerbation of UC-like chronic disease. Therefore, γδ T cells may represent a promising therapeutic target for the treatment of human UC.**

T cell receptor (TCR) γδ T cells are an evolutionary conserved T-cell subset with characteristic properties.[1] TCRγδ-bearing murine dendritic epidermal T cells are involved in the regulation of epidermal integrity and promote wound repair of the skin,[2] whereas intestinal intraepithelial γδ T cells (γδ-IEL) regulate intestinal epithelial homeostasis.[3,4] Recent evidence suggests that γδ T cells are also important in immune surveillance of the epithelium by providing a first line of defense against infectious pathogens attacking the surfaces of the body and in the regulation of linking of innate and acquired immunity.[1,5] Furthermore, γδ T cells appear to down-regulate αβ T cell-driven robust immune responses that often result in severe immunopathology.[1]

The incidence of inflammatory bowel diseases (IBD), namely ulcerative colitis (UC) and Crohn's disease (CD), has increased markedly in recent years. The factors including genetic predisposition, environmental conditions, and aberrant immune response driven by normal intestinal flora are vital for the development and persistence of the inflammatory process.[6,7] In the present study, we aimed at elucidating the role of γδ T cells in the pathogenesis of IBD because there is growing evidence supporting that γδ T cells play an active multifaceted immunoregulatory role in the coordinated innate and acquired immune responses that maintain the integrity of epithelial tissues[1,2,4,5,8] and an increase in γδ T cells in the diseased mucosa has been documented in UC patients.[9,10] In acute colitis induced by administration of either 2,4,6-trinitrobenzene sulfonic acid[11,12] or dextran sulfate sodium,[13,14] a protective role of γδ T cells has been demonstrated. However, the role of γδ T cells in chronic intestinal inflammation resembling UC has not yet been investigated. TCRα$^{-/-}$ (α$^{-/-}$) mice spontaneously develop chronic colitis with several features of human UC including a significant increase in γδ T cells.[15] To illuminate the role of γδ T cells in the pathogenesis of UC-like colitis in α$^{-/-}$ mice, we generated TCRγ$^{-/-}$

Abbreviations used in this paper: **α$^{-/-}$, TCRα$^{-/-}$; ARP, anorectal prolapse; γ$^{-/-}$, TCRγ$^{-/-}$; γδ T cells, TCR γδ T cells; IBD, inflammatory bowel disease; IEL, intestinal intraepithelial T lymphocytes; LP, lamina propria; TCR, T-cell receptor; UC, ulcerative colitis.**

0016-5085/08/$34.00
doi:10.1053/j.gastro.2007.11.056

($\gamma^{-/-}$) mice and examined the severity of colitis in $\alpha^{-/-}$ mice that are genetically engineered to lack γδ T cells.

Materials and Methods

Mice

We newly generated $\gamma^{-/-}$ mice and crossed with $\alpha^{-/-}$ mice[16] to develop double mutant ($\alpha^{-/-} \times \gamma^{-/-}$) mice. The generations of these mice are described in Supplementary Materials (see Supplemental Materials online at www.gastrojournal.org). All mice used were of C57BL/6 (B6) background. The mice were maintained under specific pathogen-free conditions, and all animal procedures described in this study were performed in accordance with the guidelines for animal experiments of Keio University School of Medicine, Yakult Central Institute for Microbiological Research, Kinki University School of Medicine, and Massachusetts General Hospital.

Flow Cytometry and Immunohistochemical Procedures

Methods for isolation of intestinal intraepithelial T cells (IEL) from mouse small intestines and lamina propria (LP) cells from mouse and human large intestines are described in Supplementary Materials. Procedures of cell staining for flow cytometric and immunohistochemical analyses are also described in Supplementary Materials (see Supplemental Materials online at www.gastrojournal.org).

Histologic Evaluation of Colitis

The disease score of colitis (0-10) was estimated in a blind fashion using previously described criteria, namely, a combination of both gross and histologic findings.[17] The gross score was rated as 0, presence of normal beaded appearance; 1, absence of beaded appearance of colon; 2, focally thickened colon; and 3, marked thickness of entire colon. The histologic score was based on the extent of intestinal wall thickening (0-3), inflammatory cell infiltration into LP (0-3), and presence (0 or 1) of ulceration.

Real-Time Reverse-Transcription Polymerase Chain Reaction Analysis

Total RNA was extracted from half of the frozen colonic tissue obtained from each one of wild-type (WT), $\gamma^{-/-}$, $\alpha^{-/-}$, and $\alpha\gamma^{-/-}$ littermate mice, and complementary DNA (cDNA) was prepared. Quantitative real-time reverse-transcription polymerase chain reaction (RT-PCR) was conducted to assess the expression level of TNF-α, IL-1β, IL-6, TGF-β, IFN-γ, IL-7, IL-10, IL-12, KC, MIP-2, GCP-2, MCP-1, MIP-1α, MIP-1β, and HPRT genes using TaqMan probes (Applied Biosystems, Foster City, CA). The relative expression level of genes of interest was normalized to the HPRT gene expression. The detailed procedures are described in Supplementary Materials (see Supplemental Materials online at www.gastrojournal.org).

Measurement of Cytokines and Chemokines by Enzyme-Linked Immunosorbent Assay

Proteins were extracted from the above-described half of the frozen colonic tissue obtained from each one of WT, $\gamma^{-/-}$, $\alpha^{-/-}$, and $\alpha\gamma^{-/-}$ littermate mice. In brief, frozen colonic tissue was homogenized with a sonicator (Ultrasonic Disruptor UD-201, TOMY, Tokyo, Japan) in 5 mL lysis buffer (50 mmol/L Tris-HCl, pH 7.4, 150 mmol/L NaCl, 1% NP-40, 1 mmol/L dithiothreitol, 1 mmol/L EDTA, 1 mmol/L NaF, 1 mmol/L sodium orthovanadate, and complete, Mini EDTA-free proteinase inhibitor [Roche Applied Science, Mannheim, Germany]), the homogenate was clarified by centrifugation at 14,000 rpm for 10 minutes, and the supernatant was subjected to OptEIA ELISA (BD Biosciences, San Diego, CA) for detection of tumor necrosis factor (TNF)-α, interleukin (IL)-1β, and IL-6 and to DuoSet ELISA (R&D Systems, Minneapolis, MN) for detection of transforming growth factor (TGF)-β, interferon (IFN)-γ, keratinocyte-derived chemokine (KC), macrophage inflammatory protein (MIP)-2 and granulocyte chemotactic protein (GCP)-2. Levels in the supernatants were standardized to the total amount of protein in the same supernatants assessed by RC DC Protein Assay (Bio-Rad Laboratories, Hercules, CA).

Chemotaxis Assay

The assays were performed using the ChemoTx 96-well plate No. 101-3 (NeuroProbe, Gaithersburg, MD). Briefly, bone marrow cells collected from femurs, tibias, and humerus of WT mice were recovered by centrifugation at the interphase of 44% and 70% Percoll solutions. Subsequently, 2.5×10^5 bone marrow cells were loaded onto the membrane plate and placed on a flat-bottomed, 96-well microtiter plate containing the colon extracts (0.7 mg protein/mL) from WT, $\alpha^{-/-}$, and $\alpha\gamma^{-/-}$ mice in addition to serially diluted MIP-2 and MCP-1 (R&D Systems). To identify the neutrophils and monocytes, bone marrow cells were labeled with fluorescent dye conjugated monoclonal antibodies (mAb) to Mac-1 and Ly-6C before the assay. After incubation at 37°C for 2 hours, the number of Mac-1^+Ly-$6C^{low}$ neutrophils[18] and Mac-1^+Ly-$6C^{high}$ monocytes[18] that migrated into the lower wells was determined by a flow cytometry.

Cell Transfer

γδ T cells were purified from the mesenteric lymph nodes (MLNs) and colon of $\alpha^{-/-}$ mice through MACS system, and 2×10^6 purified cells were intravenously transferred twice into $\alpha\gamma^{-/-}$ mice (n = 16) at 4 and 5 months of age. As control group, phosphate-buffered saline (PBS) was intravenously administrated into $\alpha\gamma^{-/-}$ mice (n = 15). The recipient mice were then killed at 6 months of age.

Statistical Analysis

The statistical difference was determined by 2-sided Student *t* test. For the statistical analysis of cell infiltration into the large intestine, 2-sided Mann–Whitney *U* test was used. Difference with $P < .05$ was considered significant.

Results

Generation of TCRγ-Deficient Mice

To begin with, we initially confirmed that γδ T cells were increased in the lymphoid cells isolated from the inflamed colonic mucosa of UC patients as compared with those from the unaffected colonic mucosa of patients with colon cancer (Figure 1*A* and *B*) and also in the lymphoid cells isolated from the inflamed colonic LP of $\alpha^{-/-}$ mice as compared with those from normal colonic LP of age-matched WT littermate mice (Figure 1*C* and *D*).

Precise appreciation of the role of γδ T cells in pathogenesis of colitis in $\alpha^{-/-}$ mice requires the generation of $\alpha^{-/-}$ mice deficient in γδ T cells. However, the previously generated TCRδ$^{-/-}$ ($\delta^{-/-}$) mice[19] lacking γδ T cells could not be used for this purpose because of the genomic localization of TCRδ coding segments within the *V* and *J* segments of TCRα gene.[20] To overcome this difficulty, we newly generated TCRγ$^{-/-}$ mice by disrupting the genes encoding TCR Cγ1, 2, 3, and 4 (CγΔ) using the Cre/*loxP* site-specific recombination system shown in Figure 2. The targeting vector pCγ4ΔNL carrying a *loxP*-flanked *pgk-neo* gene cassette in place of exon 1 of the Cγ4 gene (Figure 2*A*) was introduced into the embryonic stem (ES) clone Vγ6ΔL carrying the allele in which the Vγ6 region was replaced by a single *loxP* site (Figure 2*B*). Transfected cells were cultured in the presence of G418, and G418-resistant recombinant clones showing the joint transmission of Vγ6ΔL and Cγ4ΔNL genes were selected. These ES clones, including the clones carrying both transgenes on the same chromosome, Vγ6ΔL-Cγ4ΔNL (Figure 2*C*), were injected into B6 blastocysts. The chimeric mice obtained were crossed to the CAG-*cre* transgenic B6 mice to generate the Cγ1-, 2-, 3-, and 4-depleted TCRγ-deficient (CγΔ) allele (Figure 2*C*) by *cre*-mediated recombination in F_1 mice during embryonic development.

Subsequently, these F_1 mice were intercrossed to produce homozygous ($\gamma^{-/-}$) mice (Figure 2*D*), and these mutant $\gamma^{-/-}$ mice were backcrossed 8 times to B6 mice to obtain $\gamma^{-/-}$ mice carrying the B6 background. WT ($\alpha^{+/-} \times \gamma^{+/-}$), $\gamma^{-/-}$ ($\alpha^{+/-} \times \gamma^{-/-}$), $\alpha^{-/-}$ ($\alpha^{-/-} \times \gamma^{+/-}$), and $\alpha\gamma^{-/-}$ ($\alpha^{-/-} \times \gamma^{-/-}$) littermate F_2 mice were then produced by intercrossing $\alpha^{-/-}$ mice[16] with $\gamma^{-/-}$ mice. Flow cytometric analysis of IEL from the small intestine confirmed that γδ T cells were absent in $\gamma^{-/-}$ and $\alpha\gamma^{-/-}$ mice (Figure 2*E*).

Pathogenic Role of γδ T Cells in UC-Like Colitis

Histologic examination of the colons from 20- to 32-week-old $\alpha^{-/-}$ and $\alpha\gamma^{-/-}$ mice revealed that inflam-

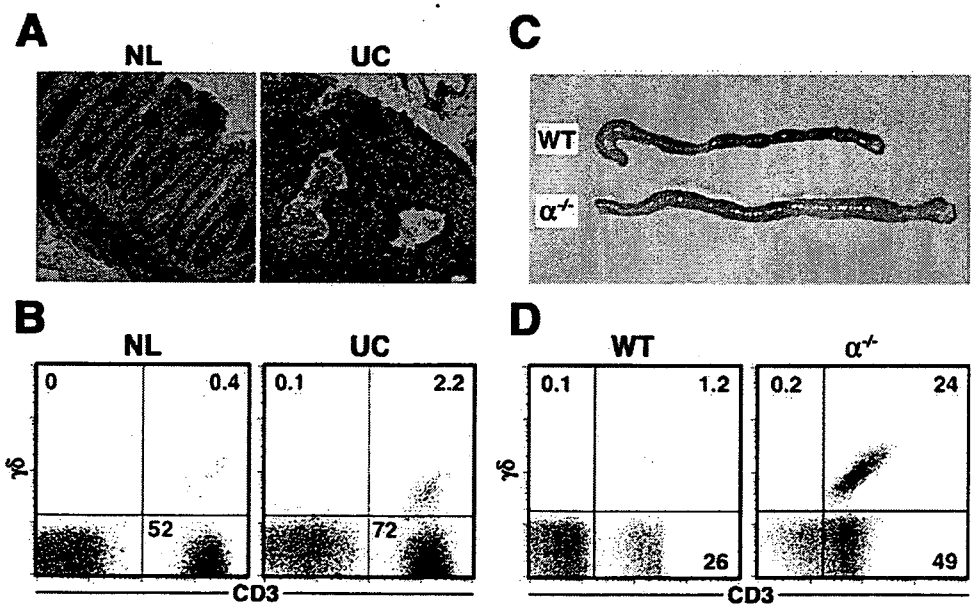

Figure 1. γδ T cells concentrate in the inflamed colonic mucosa of UC patients and colonic LP of $\alpha^{-/-}$ mice suffering from spontaneous chronic colitis. (*A*) A representative colonic tissue section from an ulcerative colitis (*UC*) patient shows a marked infiltration of lymphomyeloid cells, mucosal distortion, crypt abscess, and depletion of goblet cells compared with a normal colonic tissue section (*NL*) (original magnification, ×100). (*B*) A flow cytometry shows increased γδ T-cell population in a diseased colonic LP of UC patient compared with that in a normal colonic LP. This is a representative result of 3 UC patients. (*C*) Large intestines from wild-type (*WT*) mice and $\alpha^{-/-}$ mice suffering from spontaneous chronic colitis are shown. (*D*) A flow cytometry shows increased γδ T-cell population in a diseased colonic LP of $\alpha^{-/-}$ mice compared with that in colonic LP of WT littermate.

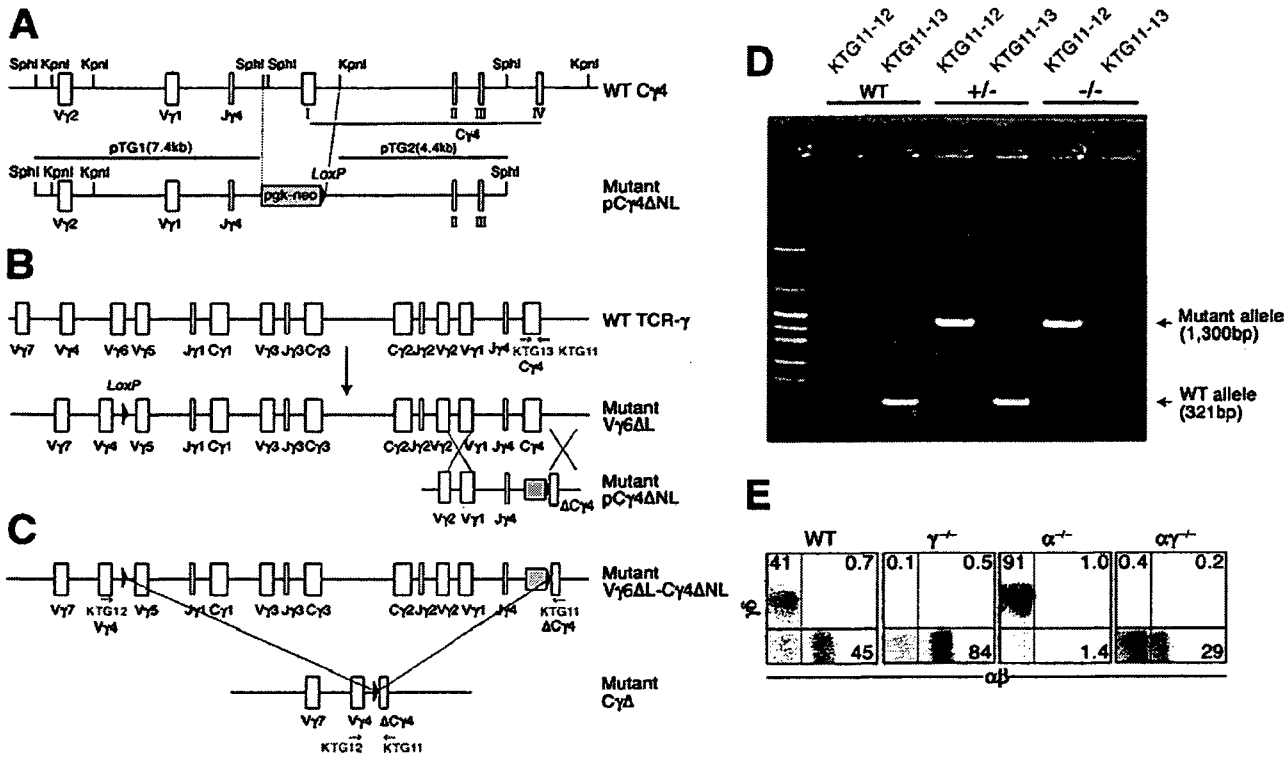

Figure 2. Generation of TCRγ-deficient mice and subsequent production of TCRαγ double mutant mice. (*A*) Schematic representation of WT and mutant (pCγ4ΔNL) genomic Cγ4 loci together with the 3 DNA fragments used to construct the mutant pCγ4ΔNL vector. The resulting targeting vector (pCγ4ΔNL) carrying a *loxP*-flanked *pgk-neo* gene cassette in place of exon 1 of Cγ4 gene used a neomycin resistance gene driven by the *pgk* promoter as positive selection marker is shown. Restriction enzyme sites, *SphI* and *KpnI* (*solid bars*), exon structures, Vγ and Jγ (*open boxes*), and *loxP* site (*solid triangle*) are indicated. (*B*) Schematic representation of the ES clone carrying WT TCRγ gene and mutant Vγ6ΔL ES clone carrying the allele in which the Vγ6 region was replaced by a single *loxP* site and mutant pCγ4ΔNL targeting vector. Exon structures, Vγ and Jγ (*open boxes*) and *loxP* site (*solid triangle*) are indicated. (*C*) Schematic representation of generation of the mutant mice that carry the TCRγ-deficient (CγΔ) allele by Cre-mediated recombination during embryonic development. Exon structures, Vγ and Jγ (*open boxes*), and *loxP* site (*solid triangle*) are indicated. (*D*) The mutant mice that carry the TCRγ-deficient (CγΔ) allele were intercrossed to produce TCRγ$^{+/+}$ (WT), TCRγ$^{+/-}$ (γ$^{+/-}$), and TCRγ$^{-/-}$ (γ$^{-/-}$) mice, and the corresponding WT and mutant alleles were typed by PCR analysis of tail DNA with each set of primers indicated. (*E*) γδ T cells are absent from the IEL compartment of γ$^{-/-}$ and αγ$^{-/-}$ mice. γ$^{-/-}$ Mice were crossed with α$^{-/-}$ mice to obtain WT (α$^{+/-}$ × γ$^{+/-}$), γ$^{-/-}$ (α$^{+/-}$ × γ$^{-/-}$), α$^{-/-}$ (α$^{-/-}$ × γ$^{+/-}$), and αγ$^{-/-}$ (α$^{-/-}$ × γ$^{-/-}$) littermate mice.

mation characterized by elongation of crypts was much milder in αγ$^{-/-}$ mice as compared with α$^{-/-}$ mice (Figure 3*A*). Although the body weight was comparable between αγ$^{-/-}$ and α$^{-/-}$ mice, it was evident that colonic weight was significantly decreased in αγ$^{-/-}$ mice as compared with α$^{-/-}$ mice (Figure 3*B*). The disease score characterized by the thickening of colonic mucosa with crypt elongation and inflammatory cell infiltration was also significantly lower in αγ$^{-/-}$ mice than that rated in α$^{-/-}$ mice (Figure 3*C*). Although approximately 20% of 20- to 60-week-old α$^{-/-}$ mice displayed anorectal prolapse (ARP), it was not discerned in any of age-matched αγ$^{-/-}$ mice (Figure 3*D*). Notably, no difference was observed in the age of onset of colitis and in the incidence of colitis (~80%) among 20- to 32-week-old αγ$^{-/-}$ and α$^{-/-}$ mice. In addition, in comparison with administration of PBS (as control), adoptive transfer of γδ T cells that were purified from α$^{-/-}$ mice did not increase the incidence of colitis in the recipient αγ$^{-/-}$ mice. However, the transfer of γδ T cells exacerbated the severity of colitis in the recipient αγ$^{-/-}$ mice. As shown in Figure 3*E*, more severe inflammatory cell infiltration was observed in the inflamed colon of the recipient αγ$^{-/-}$ mice with γδ T-cell transfer as compared with control αγ$^{-/-}$ mice. Therefore, it is possible that γδ T cells may be involved in the exacerbation, but not induction, of UC-like colitis.

Decrease in the Colonic Neutrophils and Monocytes in the Absence of γδ T Cells

The above results indicate that the spontaneous colitis in α$^{-/-}$ mice is ameliorated by the absence of γδ T cells in αγ$^{-/-}$ mice. With these findings in mind, flow cytometric analysis of colonic LP cells isolated from WT, γ$^{-/-}$, α$^{-/-}$, and αγ$^{-/-}$ littermate mice at approximately 28 weeks of age was performed, and the representative results of 5 independent experiments are presented in Figure 4*A*. In this experiment, WT, γ$^{-/-}$, α$^{-/-}$, and αγ$^{-/-}$ littermate mice yielded 5.1 × 10^5, 6.1

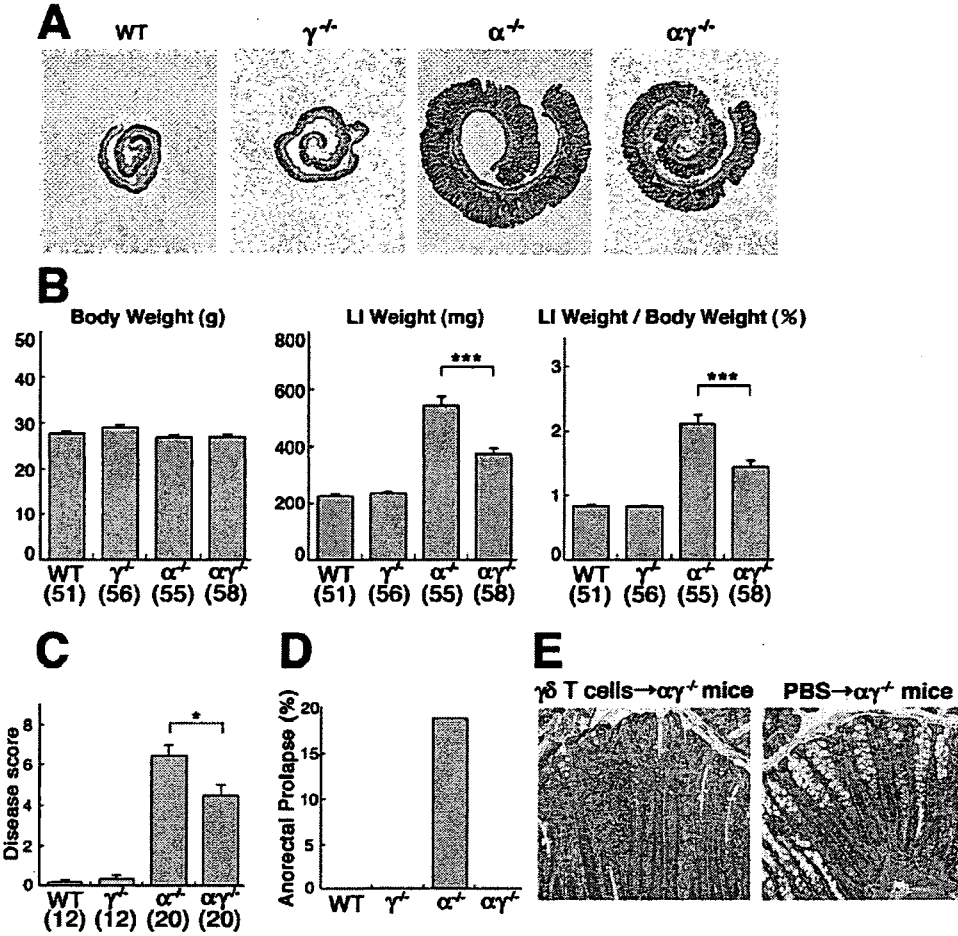

Figure 3. Colonic mucosal inflammation is milder in $\alpha\gamma^{-/-}$ mice lacking γδ T cells than in $\alpha^{-/-}$ mice possessing γδ T cells. (*A*) Representative histologic pictures of colon from WT, $\gamma^{-/-}$, $\alpha^{-/-}$, and $\alpha\gamma^{-/-}$ littermate mice. These mice were maintained in the same cages under specific pathogen-free conditions and examined at 28 weeks of age. (*B*) Body weight, wet weight of large intestine (LI weight), and ratio (%) of LI weight to body weight in WT, $\gamma^{-/-}$, $\alpha^{-/-}$, and $\alpha\gamma^{-/-}$ littermate mice at 20 to 32 weeks of age are shown. Values in parentheses are numbers of mice examined. $^{***}P < .001$. (*C*) Disease scores (0–10) of colitis in 24- to 32-week-old WT, $\gamma^{-/-}$, $\alpha^{-/-}$, and $\alpha\gamma^{-/-}$ mice were assessed. Values in parentheses are numbers of mice examined. $^{*}P < .05$. (*D*) Incidence of ARP in 24- to 60-week-old WT, $\gamma^{-/-}$, $\alpha^{-/-}$, and $\alpha\gamma^{-/-}$ mice. (*E*) The histologic findings (original magnification, ×20) of colon of recipient $\alpha\gamma^{-/-}$ mouse groups that received transfer of γδ T cells (*left panel*) and that received PBS (*right panel*).

× 10^5, 32.3 × 10^5, and 12.0 × 10^5 colonic LP cells, respectively. Based on the absolute numbers of infiltrated cells and the flow cytometry results shown in Figure 4*A*, it was evident that fewer Mac-1$^+$Ly-6G$^-$ cells and Mac-1$^+$Ly-6G$^+$ cells were present in the colonic LP cell population of $\alpha\gamma^{-/-}$ mice as compared with those of $\alpha^{-/-}$ mice. Monocytes express Mac-1 but not Ly-6G, whereas neutrophils express both Mac-1 and Ly-6G.[21] Therefore, our results suggest that, in addition to monocyte infiltration (Figure 4*A*), there is a marked infiltration of neutrophils in the inflamed colonic LP of $\alpha^{-/-}$ mice. We also confirmed our previous finding[15] that a remarkable increase in γδ T cells was observed in the inflamed colonic LP of $\alpha^{-/-}$ mice (Figure 4*A*).

Immunohistochemical examination of inflamed colons from $\alpha^{-/-}$ and $\alpha\gamma^{-/-}$ mice at approximately 28 weeks of age was performed to further confirm flow cytometric results. Consistent with the flow cytometric observations, significantly smaller numbers of Mac-1$^+$ cells and Ly-6G$^+$ cells were observed in the colonic LP of $\alpha\gamma^{-/-}$ mice as compared with those in the colonic LP of $\alpha^{-/-}$ mice (Figure 4*B*).

To investigate whether γδ T cells contribute to the generation of colonic environment for enhancing the migration of neutrophils and monocytes into the inflamed colon, we examined chemotactic activity of colonic extracts from $\alpha^{-/-}$ and $\alpha\gamma^{-/-}$ mice to neutrophils and monocytes (Figure 5*A*). As a result, chemotactic activity to neutrophils of colonic extracts from $\alpha\gamma^{-/-}$ mice was significantly weaker than that from $\alpha^{-/-}$ mice, whereas the chemotactic activities to monocytes of both extracts were almost comparable (Figure 5*B*). The marked infiltration of neutrophils into the inflamed colonic LP of $\alpha^{-/-}$ mice is most likely mediated by some factors, such as MIP-2 (Figure 5*A*), that are enhanced in the presence of γδ T cells.

Taking all of these results together, and in conjunction with our previous findings,[22] colonic γδ T cells of $\alpha^{-/-}$ mice exert aggravating effect on the UC-like colitis by increasing primarily the influx of neutrophils into the inflamed mucosa.

Attenuation of Colonic Proinflammatory Cascades by the Absence of γδ T Cells

In view of the severe colitis, increased infiltration of Mac-1$^+$Ly-6G$^+$ and Mac-1$^+$Ly-6G$^-$ cells, and marked production of neutrophil chemotactic factor(s) in the inflamed colonic LP of $\alpha^{-/-}$ mice, quantitative real-time